

Design of a Variable Valve Actuation System
For an Automobile Engine

A Final Year Project Report

Presented to

SCHOOL OF MECHANICAL & MANUFACTURING ENGINEERING

Department of Mechanical Engineering

NUST

ISLAMABAD, PAKISTAN

In Partial Fulfillment

Of the Requirements for the Degree of
Bachelors of Mechanical Engineering

By

Muhammad Shamir Shahid

Muhammad Nauman Tariq

Muhammad Mubashir

Muhammad Shaheer Khan

June 2021

EXAMINATION COMMITTEE

We hereby recommend that the final year project report prepared under our supervision by:

Muhammad Shamir Shahid	217124
Muhammad Nauman Tariq	210655
Muhammad Mubashir	217124
Muhammad Shaheer Khan	218127

Titled: “Design of a Variable Valve Actuation System for an Automobile Engine” be accepted in partial fulfillment of the requirements for the award of Bachelors of Mechanical Engineering degree with grade ____

Supervisor: Dr. Sami Ur Rehman, Assistant Professor SMME, NUST	_____ Dated:
Committee Member: Dr. Jawad Aslam, Assistant Professor SMME, NUST	_____ Dated:
Committee Member: Dr. Sana Waheed, Assistant Professor SMME, NUST	_____ Dated:

(Head of Department)

(Date)

COUNTERSIGNED

Dated: _____

(Dean / Principal)

ABSTRACT

Due to the continuous increase in global warming and pollution around the world, there is an increase need of reducing CO₂ emissions that harm the environment. Automobiles are one of the major contributors to the damage of ozone layer and yet they are a basic necessity for human life. Even though car companies are making a move for electric vehicles that have no contribution to global warming, they still have a long way to go. Petrol and diesel vehicles are to stick around for the considerable future due to the fact that electric vehicles are expensive and the technology is still in development. So hence, there is a need to modify the current petrol & diesel engines so that they contribute less to the pollution. Our project is aimed at creating a variable valve actuation system that will do just that by reducing the CO₂ emissions along with increasing the efficiency, power, fuel economy and also eliminate the camshaft from the engine which will result in a smaller engine and will give us much more control over the engine's performance.

Key Words: Variable actuation system, camshaft, engine performance.

ACKNOWLEDGEMENTS

We are thankful to our Creator Allah for providing us an opportunity to study at the prestigious institution and working on this project. Allah gave us perseverance and strength to get this project done. We are grateful for the help and guidance. Whoever helped us through the course of this project, whether our parents, teachers, supervisors or any other individual was His will, so indeed none be worthy of praise but Him.

We are profusely thankful to our beloved parents who raised us when we were not capable of walking and continued to support us throughout in every department of our lives.

Our team acknowledges the contributions of the team at Freevalve Technology & Koenigsegg who have laid the foundation for workings of the camless engine and pneumatically controlled variable valve actuation system.

We would also like to express special thanks to our supervisor Dr. Sami our Rehman for his help throughout our thesis and also for Internal Combustion Engines, Thermodynamics – I and Machine Design courses which he has taught us.

We would also like to thank Dr. Jawad Aslam and Dr. Sana Waheed, for being on our thesis guidance and evaluation committee. Their critical analysis of our progress paved a way for this successful completion of the thesis.

Finally, we would like to express our gratitude to all the individuals who have rendered valuable assistance to our study.

“Dedicated to our exceptional parents and adored siblings whose tremendous support and cooperation led us to this wonderful accomplishment.”

ORIGINALITY REPORT

1111

ORIGINALITY REPORT

15%

SIMILARITY INDEX

13%

INTERNET SOURCES

6%

PUBLICATIONS

8%

STUDENT PAPERS

PRIMARY SOURCES

1	www.electronics-tutorials.ws Internet Source	1%
2	www.atlantis-press.com Internet Source	1%
3	kth.diva-portal.org Internet Source	1%
4	www.rixufangshui.com Internet Source	1%
5	Submitted to Higher Education Commission Pakistan Student Paper	1%
6	docplayer.net Internet Source	1%
7	article.sciencepublishinggroup.com Internet Source	1%
8	link.springer.com Internet Source	1%
9	tameson.co.uk Internet Source	<1%

COPYRIGHTS

The design and development of the Variable Valve Actuation System, its properties and specifications, and all related material are the intellectual property of the student authors: MUHAMMAD SHAMIR, MUHAMMAD NAUMAN TARIQ, MUHAMMAD MUBASHIR and MUHAMMAD SHAHEER KHAN, the institution: SCHOOL OF MECHANICAL AND MANUFACTURING ENGINEERING of the NATIONAL UNIVERSITY OF SCIENCES AND TECHNOLOGY, ISLAMABAD.

Any unauthorized use of the research, the design and all pertaining elements will result in copyright infringement of the material and the authors and involved parties will have every right to take legal action against the perpetrator/s.

TABLE OF CONTENTS

ABSTRACT.....	3
ACKNOWLEDGEMENTS.....	4
ORIGINALITY REPORT	6
COPYRIGHTS	7
LIST OF FIGURES	12
LIST OF TABLES	14
ABBREVIATIONS	15
NOMENCLATURE	17
Chapter 1 : INTRODUCTION.....	18
1.1 Motivation.....	18
1.2 Need	18
1.3 Objectives	19
Chapter 2 : LITERATURE REVIEW.....	20
2.1 Internal Combustion Engine.....	20
2.1.1 Camshaft	20
2.2 CAMLESS ENGINES	21
2.3 CAM VS CAM-LESS ENGINES.....	23

2.4	TYPES OF CAMLESS SYSTEMS	25
2.4.1	Electro-Magnetic Valve Actuation System (EMVA):.....	25
2.4.2	Electrohydraulic Valve Actuation (EHVA):.....	25
2.4.3	Electro-Pneumatic Valve Actuation (EPVA):	26
2.5	VARIABLE VALVE ACTUATION.....	27
2.5.1	Timing:.....	28
2.5.2	Lift.....	29
2.5.3	Duration	30
2.6	PNEUMATIC ACTUATORS	31
2.6.1	Single acting Actuator.....	31
2.6.2	Double Acting Actuator	32
2.7	SPOOL VALVE.....	35
2.8	4/3 WAY DIRECTIONAL VALVE.....	35
2.8.1	VALVE CONFIGURATION OF 4/3 DCV	36
2.9	SOLENOID	38
2.9.1	Solenoid Coil's Magnetic Field	39
2.9.2	Construction of Pull-Type Solenoid	40
2.9.3	Modelling of a Solenoid.....	40
2.10	MODELLING OF A VALVE.....	43

2.11	FLOW FORCES.....	43
2.11.1	ORIFICE AREA	44
Chapter 3 : METHODOLOGY.....		46
3.1	ACQUIRING ENGINE DATA	46
3.2	SVAJ DIAGRAMS.....	47
3.3	VALVE TRAIN DYNAMICS	48
3.4	DESIGN.....	52
3.5	SIMULATION AND SIMULINK ANALYSIS.....	57
3.6	SOLENOID AND DCV SELECTION.....	63
3.7	STRUCTURAL ANALYSIS	65
3.8	CFD ANALYSIS	66
Chapter 4 : RESULTS		69
4.1.	PARAMETRIC AND GRAPHIC RESULTS	69
4.2	SIMULINK DISCUSSION	79
4.3	CFD Discussion	79
4.4	FEM Discussion.....	80
Chapter 5 : MANUFACTURING PLAN		82
5.1	Manufacturing Processes	82
5.2	Pneumatic Components	84

5.3 Sensors	86
5.3.1 Position Sensors	86
5.3.2 Optical Encoder	87
5.3.3 Pressure Sensor	88
5.4 Cost Analysis	89
Chapter 6 : CONCLUSIONS AND RECOMMENDATIONS	90
REFERENCES	92
APPENDIX I: Sensor Technology	94
APPENDIX II: Compression Spring Specifications.....	96
APPENDIX III: CFD Convergence Results	97
APPENDIX IV: GOODMAN FAILURE DIGRAM	98

LIST OF FIGURES

Figure 1: Daihatsu Boon Engine

Figure 2: 4 Stroke SI Engine Cycle

Figure 3: Cam shaft

Figure 4: Theoretical Valve Lift Profile for CAM based system

Figure 5: Freevalve Engine

Figure 6: Koenigsigg Camless Engine

Figure 7: Theoretical Valve Lift profile for Camless System

Figure 8: Cam-based versus Camless Lift Profiles

Figure 9: Relationship between Engine Speed and Volumetric Efficiency

Figure 10: EMVA System schematic

Figure 11: Ford's EHVA system

Figure 12: Cargine's EPVVA System

Figure 13: VVT Diagram

Figure 14: Effect of VVT on engine cycle

Figure 15: Honda's VTEC System

Figure 16: Single Acting Pneumatic Actuator

Figure 17: Double Acting Pneumatic Actuator

Figure 18: Simplified DAPA

Figure 19: Double Acting Actuator

Figure 20: DCV Configurations

Figure 21: Spool Valve Positions

Figure 22: Solenoid Magnetic Field

Figure 23: Pull Type Solenoid

Figure 24: SVAJ Plots for 800 RPM

Figure 25: SVAJ Plots for 4000RPM

Figure 26: Valve Displacement Plots

Figure 27: Valve Velocity Profiles

Figure 28: Valve Acceleration Profiles

Figure 29: Design Mental Map

Figure 30: Proposed DAPA Design

Figure 31: Pressure Chamber with Excess Flow Valve

Figure 32: Actuator Housing

Figure 33: Pneumatic Circuit Schematic

Figure 34: DCV Subsystem

Figure 35: DAPA Subsystem

Figure 36: Spool Input Subsystem

Figure 37: DCV with double solenoid control

Figure 38: Spool Positions for different RPMS

Figure 39: Generated Mesh for Analysis

Figure 40: Generated Mesh for 2D Structure

Figure 41: Exploded View of Actuator

Figure 42: Pneumatic Seals

Figure 43: Optical Encoder

LIST OF TABLES

- Table 1: 1KR-FE Engine Data
- Table 2: Valve displacement functions
- Table 3: Component Materials
- Table 4: Component Masses
- Table 5: Gas Properties
- Table 6: DAPA Data
- Table 7: DCV Working Parameters
- Table 8: Pneumatic Circuit Working Conditions
- Table 9: Solenoid Data
- Table 10: Inlet Fluid Flow Conditions
- Table 11: Parametric Results 1
- Table 12: Parametric Results 2
- Table 13: Parametric Results 3
- Table 14: Quantitative FEM Results
- Table 15: Maximum Stresses and Deformation
- Table 16: Pneumatic Seal Selection
- Table 17: Position Sensor types
- Table 18: Optical Encoder Working Conditions
- Table 19: Pressure Sensor Working Conditions
- Table 20: Cost Analysis

ABBREVIATIONS

AP	Actuator Piston
BDC	Bottom Dead Center
BMEP	Brake Mean Effective Pressure
CA	Crank Angle
CAD	Crank Angle Degrees
CA50	Crank Angle for 50 % heat release (ATDC)
CI	Compression Ignition
DI	Direct Injection
DISC	Direct Injection Stratified Charge
DOHC	Double Overhead Camshaft
ECU	Electronic Control Unit
EGR	Exhaust Gas Recirculation
EPVA	Electronically controlled Pneumatic/hydraulic Valve Actuator
EV	Exhaust Valve
EVC	Exhaust Valve Closing
EVO	Exhaust Valve Opening
FVVT	Fully Variable Valve Train
HCCI	Homogeneous Charge Compression Ignition
I/O	Input/output
ICE	Internal Combustion Engine
IMEP	Indicated Mean Effective Pressure
IV	Inlet Valve
IVC	Inlet Valve Closing

IVO	Inlet Valve Opening
LS	Lift Solenoid
PI	Port Injection
PS	Position Sensor
RPM	Revolutions per Minute
SI	Spark Ignition
SPEAB	Södertälje Powertrain Engineering AB
TDC	Top Dead Center
TS	Timing Solenoid
VVT	Variable Valve Timing
DCV	Directional Control Valve

NOMENCLATURE

k	Spring constant
x	spring displacement
s	displacement
v	velocity
a	acceleration
j	jerk
m	momentum
F_v	Valve Forces
R	Resistance
I	Current
V	Voltage
A	Area
m_a	Mass Flow rate
P	Pressure
L	Length
C_d	Drag Coefficient
μ	permeability
ρ	density
f_m	magnetic force

CHAPTER 1 : INTRODUCTION

1.1 Motivation

Petrol and diesel engines are the most used in automobiles but however they are huge contributors to global warming. Due to this very reason, electric vehicles are being preferred which are expensive so hence this leads us to the conclusion that petrol engines are to stick around for the foreseeable future. Therefore, the petrol engines need to be modified to reduce their carbon footprint in order to compete with electric vehicles.



Figure 1: Daihatsu Boon Engine

1.2 Need

This project will lead to reduced carbon emissions by an automobile due to which the petrol engine will give some competition to the electric engine.

This will improve the petrol engine in the following ways:

- Better efficiency
- More power
- Better fuel economy
- Less CO₂ emissions
- Smaller size

- More control
- All the above mentioned traits signify the need for this modification if humanity wants to survive on Earth.

1.3 Objectives

The objectives of the project are as follows:

- Mathematical Calculations required to create the design
- Mechanical Design of the actuator system
- FEM and CFD analysis of the actuator system
- Generating the relevant simulations and schematics of the system.

CHAPTER 2 : LITERATURE REVIEW

2.1 Internal Combustion Engine

An internal combustion engine is a heat engine in which a specific fuel such as petrol or diesel is combusted in a chamber using an oxidizer like air. The basic principle is that the ignition causes a release of force which moves the relevant pistons a relevant distance resulting in the conversion of chemical energy to work. IC engines are characterized as two-stroke, four-stroke or six-stroke which signifies the number of strokes needed to complete a full cycle. A four-stroke IC engine completes intake, compression, combustion and exhaust strokes while turning the crankshaft. Gas turbines, jet engines and rockets are a second class of IC engines which also work on the same principle.

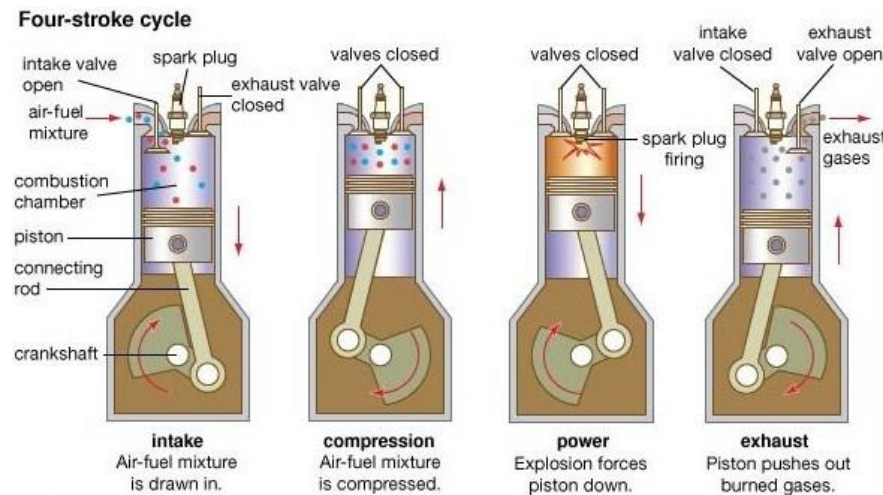


Figure 1: 4 Stroke SI Engine Cycle

2.1.1 Camshaft

Camshaft is a rotating cylindrical rod that has cams attached to it for each valve. Camshaft converts rotating motion into reciprocating motion. It is responsible for the operation of the exhaust and intake valves of an IC engine. It pushes the pistons open and close in the combustion chamber for the intake and exhaust of air which is required for the combustion process. Camshaft is usually made from steel or cast iron.



Figure 3: CAM Shaft

The theoretical valve lift profile for a cam system is observed to be the following:

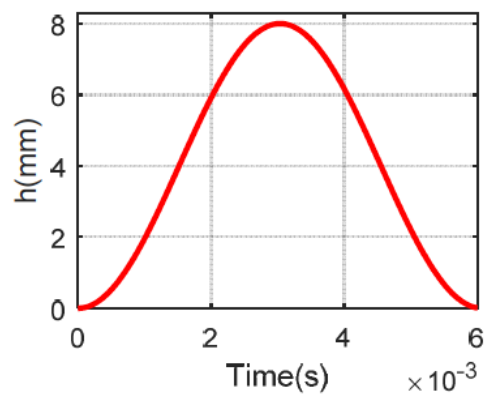


Figure 4: Theoretical Valve Lift Profile for CAM based system

2.2 CAMLESS ENGINES

A camless engine is an engine without the camshaft. The camshaft is replaced by actuators that open and close the valves of the engines. These actuator can be operated by electromagnetic, hydraulic or pneumatic means. Each actuator has their own pros and cons but pneumatic actuators are more widely used and adopted by car companies such as Koenigsegg. The conventional cam engines have restricted valve lifts and timings and adjusting that can be very difficult. However, camless engines allow for more freedom and the valve timing and valve lift can be varied infinitely from cycle to cycle. It can have multiple lift events in

a cycle or none at all which all depends on our needs and this introduces many new possibilities and potential in the engine.



Figure 5: Freevalve Engine



Figure 6: Koenigsig Camless Engine

The valve lift profile of the camless system is different due to more control over valve opening and closing. The following graph is generated to represent it:

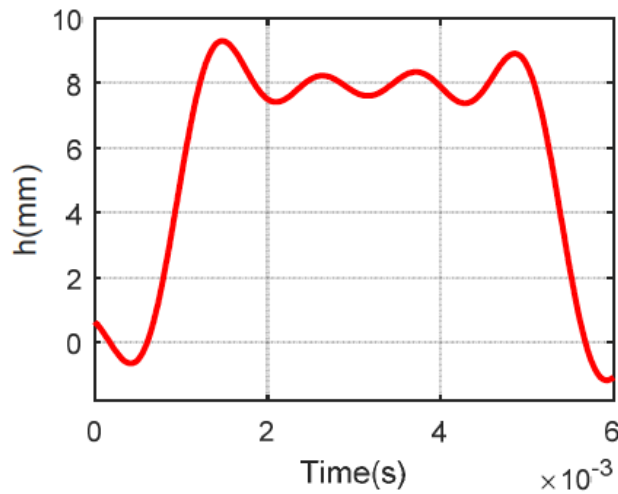


Figure 7: Theoretical Valve Lift profile for Camless System

2.3 CAM VS CAM-LESS ENGINES

As discussed above that the valve lift profiles of cam and camless systems differ a lot and the following graph compares them.

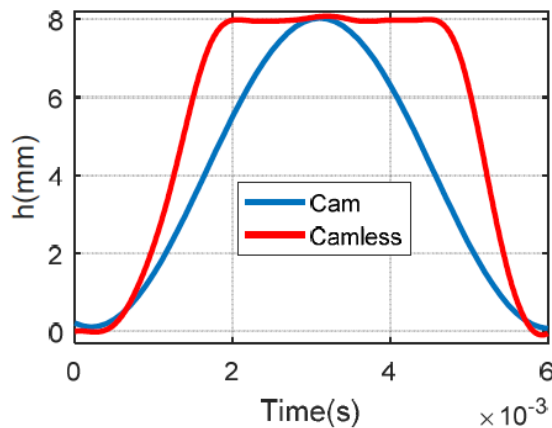


Figure 8: Cam-based versus Camless Lift Profiles

The intake system of an IC engine is made up of the air filter, carburetor, the throttle plate, intake manifold, intake port, and intake valve which all dictate the mass flow of air that an engine can induct. Hence, volumetric efficiency is the parameter that is used to measure the effectiveness of the engine's inductive process. Volumetric efficiency is the breathing capacity of an engine and is

directly related to the power generated by the engine. So in order to compare both systems, their volumetric efficiencies need to be calculated at various RPMs using the following formulas:

- For cam system,

$$\eta_c = \frac{2\rho_a v_a A_c}{\rho_a v_d N}$$

- For camless system,

$$\eta_{cl} = \frac{2\rho_a v_a A_{cl}}{\rho_a v_d N}$$

The mass flow rates are calculated using the following formula:

$$\dot{m}_a = \rho_{air} v_a A.$$

After thorough calculations at different RPMs, the following graph is drawn for comparison where it is seen that camless system has a higher volumetric efficiency:

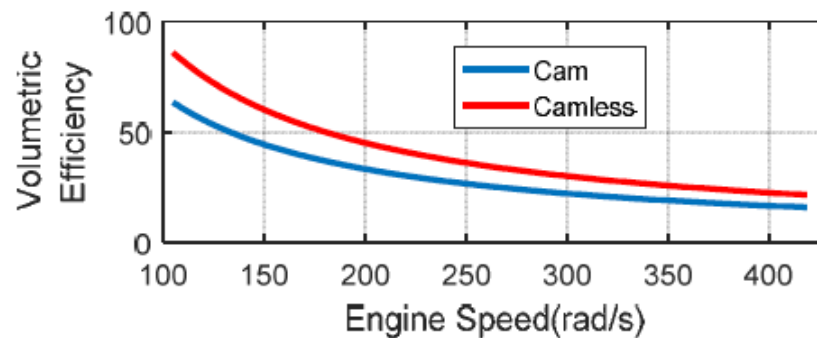


Figure 9: Relationship between Engine Speed and Volumetric Efficiency

From the above results we can come to the following conclusion:

- Camless systems have better efficiency
- Camless systems have more power output
- Camless systems have better torque
- Camless systems have better fuel economy
- Camless systems have more freedom in controlling the valve lift and valve timing

- Camless systems are smaller in size
- Camless systems have low exhaust emissions
- Camless systems have better idle stability

2.4 TYPES OF CAMLESS SYSTEMS

2.4.1 Electro-Magnetic Valve Actuation System (EMVA):

EMVA consists of two opposing permanent magnets and two opposing springs that work in parallel. The coils are connected in series due to which the current flow is in the same direction which causes an equal electromotive force on the armature during the valve stroke. The EMVA consists of stationary permanent magnets, stationary copper coils, and a moving armature made of steel, on which the valve is rigidly attached which thus transmits a bi-directional force. This system is simple but it is affected by many nonlinear phenomenon that can alter its dynamics such as friction and impacts.

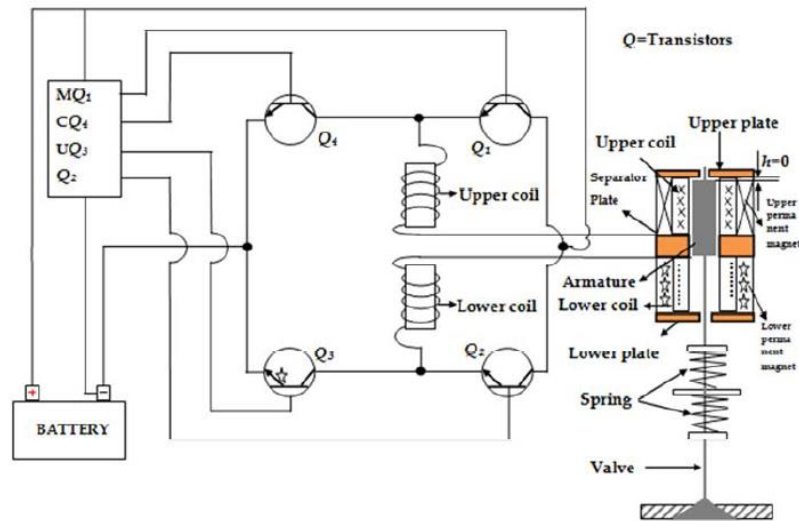


Figure 10: EMVA System schematic

2.4.2 Electrohydraulic Valve Actuation (EHVA):

EHVA is another way to actuate valves without cams. The way EHVA works is that it converts the fluid pressure into motion when a signal response is provided.

Hydraulic force is used to open and close the valves without any utilization of cams or springs. The potential energy of the compressed fluid is converted to kinetic energy which results in valve acceleration. During deceleration this energy is returned to the fluid. The high-pressure solenoid is opened when the valve is in its closed position and the high-pressure fluid is injected into the volume above the valve. The area on the on the upside of the valve is larger so the net hydraulic force is directed downwards and the valve opens. When the valve moves towards its lowest position, the high pressure solenoid closes due to which the high pressure fluid supply is also cut-off. Low pressure fluid is released which decelerates the valve until it stops at the desired valve lift.

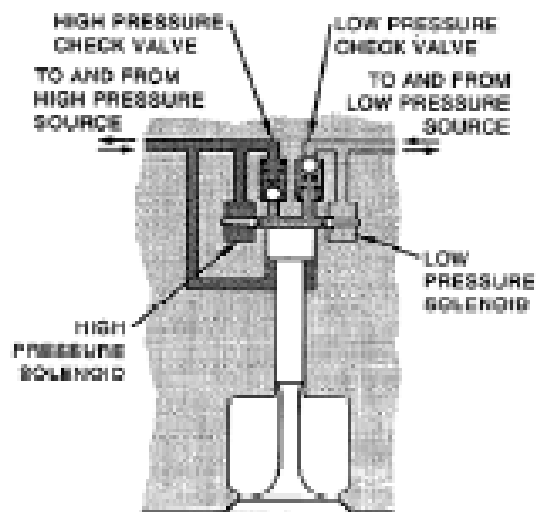


Figure 11: Ford's EHVA system

2.4.3 Electro-Pneumatic Valve Actuation (EPVA):

The pneumatic valve actuator is made up of the actuator housing, appropriate amount of spool valves, two solenoids, two port valves, a hydraulic damper, an actuation system and air flow channels within the housing. Optical sensors inside the actuator are used to receive the valve lift information.

The first step is the activation of the solenoid which pushes the corresponding spool valve to allow pressurized air inside the actuator cylinder. This pressurized air pushes the piston and opens the valve. Then, the second solenoid is activated to stop the air flow and the time difference in both the solenoids determine the valve lift. At the end the hydraulic latch is activated during the dwell period to prevent the valve from returning. After that the first solenoid is deactivated and the latch is disabled which results in air discharge and the closing of the valves. One thing to be noted is that the time difference between the second and first solenoid must be positive to prevent a second air filling of the cylinder. The damper ensures a soft-seating with a low level of noise.

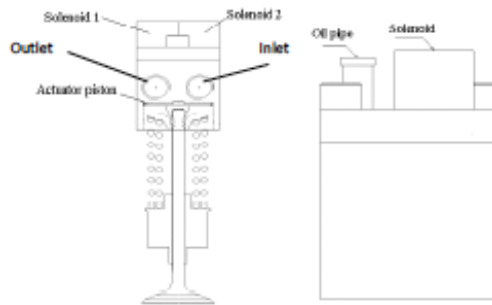


Figure 12: Cargine's EPVVA System

2.5 VARIABLE VALVE ACTUATION

Oil reserves are depleting, fuel prices are increasing, stricter emission standards have been introduced which has motivated manufacturers to development advanced power-train subsystems for better efficiency and fuel economy.

The most widely used mechanisms for actuating the engine valves are based on the modifications of the camshaft and subsequently the cam profile. The valve displacement profiles can be parametrized as follows:

2.5.1 Timing:

This parameter i.e. timing is the crank angle (CAD) at valve opening and closing with respect to the TDC or BDC.

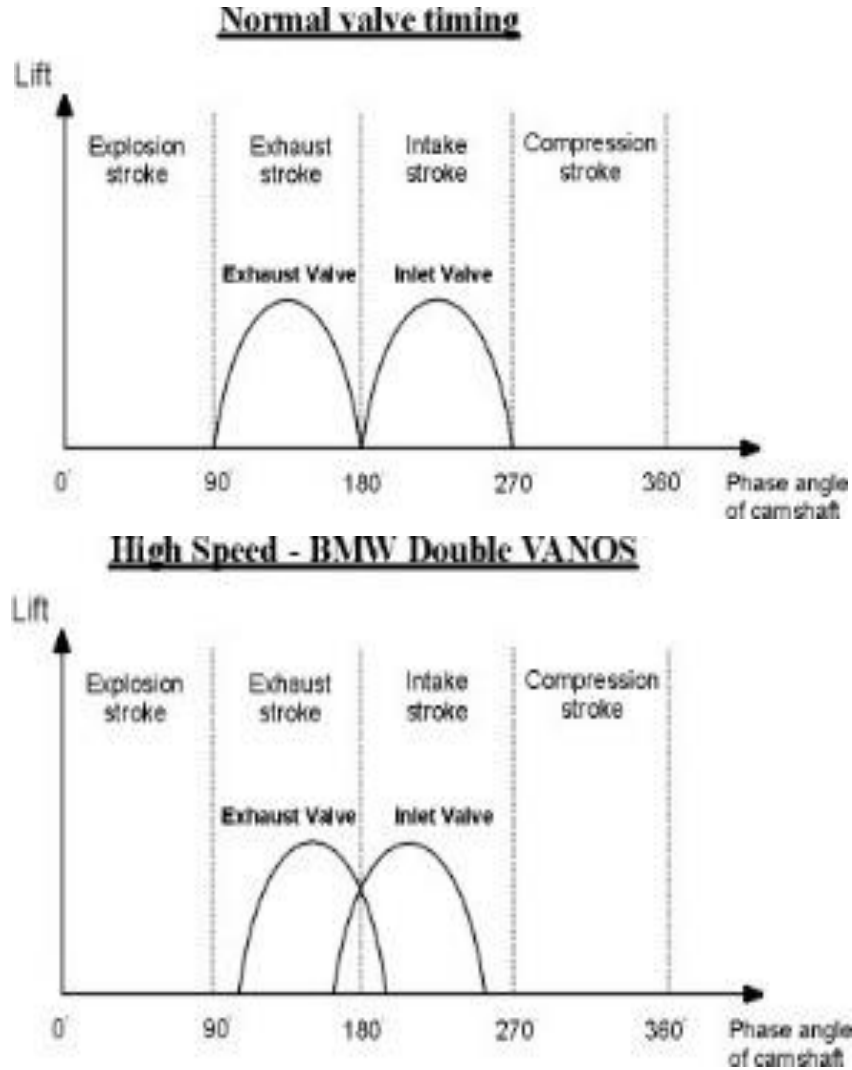


Figure 13: VVT Diagram

Valves are responsible for controlling airflow in and out of the engine. The timing of these flows are controlled by the shape and phase angle of cams. Variable Valve Timing (VVT) is the adjustment of valve timing at different speeds according to the engine's requirement to optimize the flow. The best method to optimize flow and hence reduce pumping losses is to open the inlet valves earlier and close the exhaust valves later. In other words,

the overlapping between intake valve stroke and exhaust valve stroke should be increased as RPM increases.

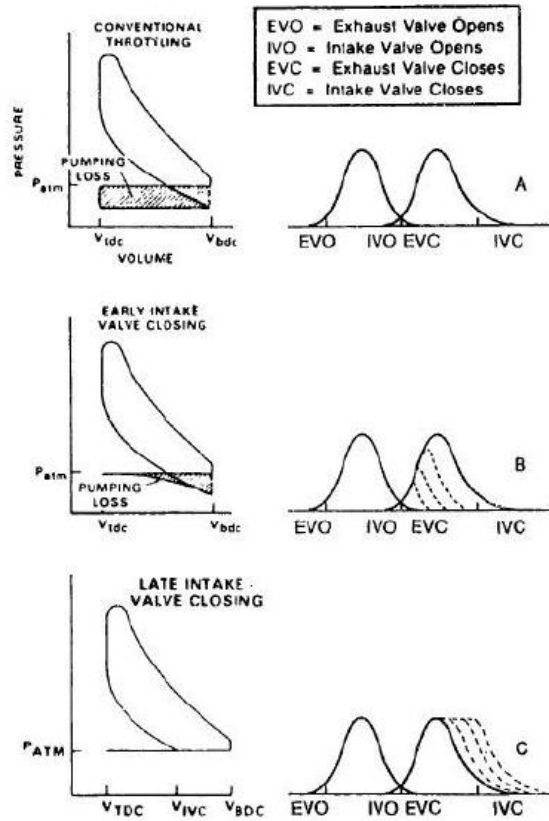


Figure 14: Effect of VVT on engine cycle

2.5.2 Lift

This parameter i.e. lift is the maximum displacement of the engine valve. Variable valve lift (VVL) is the mechanism to vary the maximum displacement of the valve in order to improve performance, fuel economy or emissions. The greater the lift, the more air flows into or out of the chamber depending on requirements of the system.

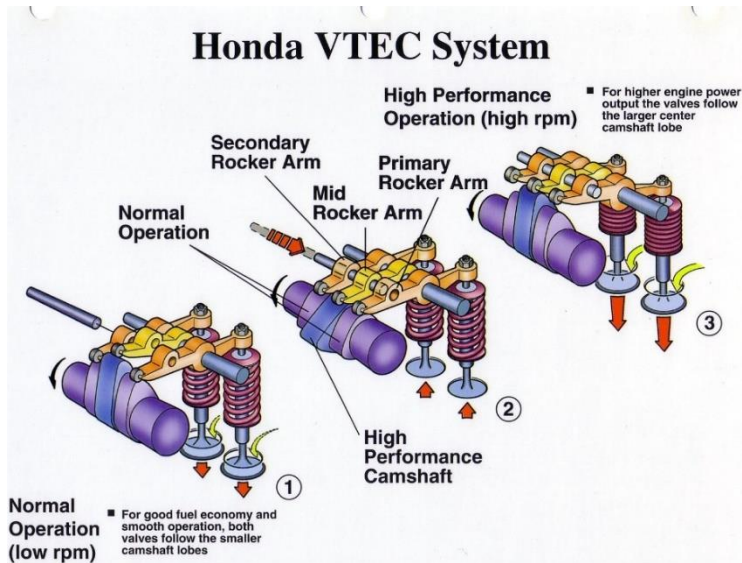


Figure 15: Honda's VTEC System

2.5.3 Duration

This parameters i.e. duration extends or shortens the period a valve is actuated from the point of opening of the valve. Variable Valve Duration (VVD) is a relatively new technology deployed by Hyundai. As intake air is relatively slower than exhaust air, it needs more time to occupy the chamber, increase in duration allows for more airflow into the chamber which leads to better combustion.

2.6 PNEUMATIC ACTUATORS

Pneumatic actuators rely on some form of pressurized gas, most often compressed air entering a chamber and causing a pressure increase. When increase in pressure is sufficient to overcome opposing forces, it results in the controlled kinetic movement of either a linear or rotary component.

Pneumatic actuators are very popular because the conversion of compressed gas into kinetic energy is very reliable, controllable and repeatable.

There are two primary varieties of pneumatic linear actuators. They both use pressurized chamber(s) to move the piston, but the main difference is the return method.

The types include:

2.6.1 Single acting Actuator

They have one port that allows air to flow in and one out of the cylinder. The pressure increase causes the piston to move forward or backward, depending on it being a push or pull type. Then a large spring returns the piston to its original position, preparing it for another cycle. To reduce seating velocity and also the impact force on the return stroke, a damping effect is used.

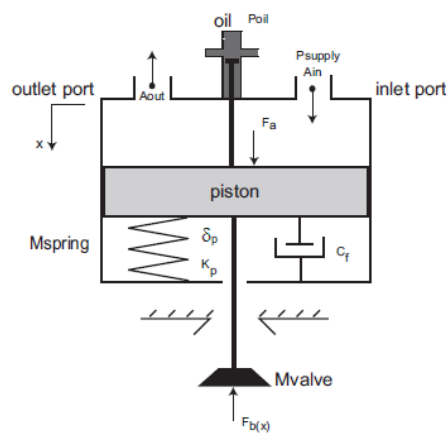


Figure 16: Single Acting Pneumatic Actuator

2.6.2 Double Acting Actuator

They have two ports and two pressure chambers, one on either side of the piston. Firstly the pressure is applied into chamber 1 which pushes the piston forward. Then, the second burst of pressure is introduced into chamber 2 on the other side of the cylinder which pushes the piston back to its neutral position. This repetitive motion leads to cyclic actuation of the piston. Usually, double-action cylinders are better for industrial uses, as they provide more force at a faster rate. They may also offer better reliability and longevity. However, they usually operate with directional control valves so they are a more expensive option in comparison.

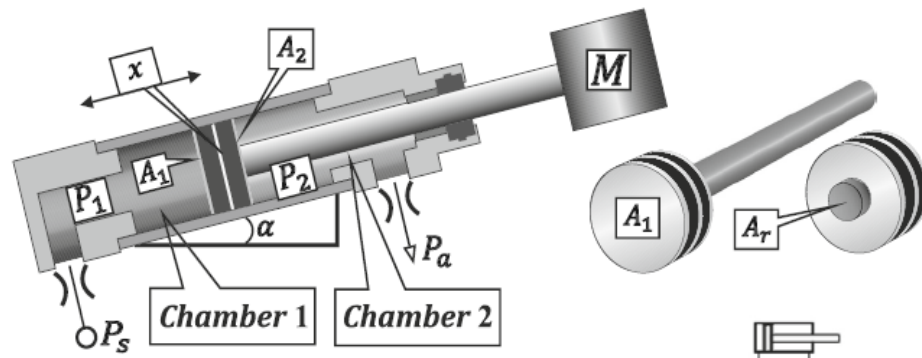


Figure 17: Double Acting Pneumatic Actuator

Looking into the double acting pneumatic actuator in detail, the mathematical model of pressure variations in each chamber is given by:

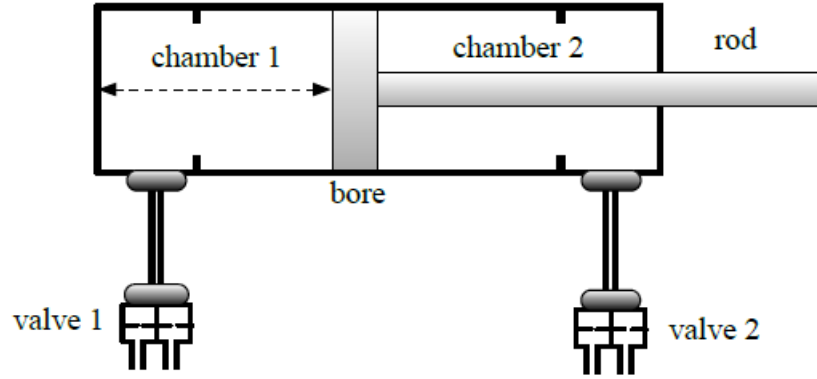


Figure 18: Simplified DAPA

$$\dot{P}_1 = \frac{C_f R \sqrt{T}}{V_{01} + A_1 \left(\frac{1}{2} L + x \right)} \left[\alpha_{in} \phi_{in1} \bar{A}_{v1in} P_s \dot{m}_r(P_s, \bar{P}_1) - \alpha_{ex} \phi_{ex1} \bar{A}_{v1ex} \bar{P}_1 \dot{m}_r(\bar{P}_1, P_a) \right] - \alpha \frac{P_1 A_1}{V_{01} + A_1 \left(\frac{1}{2} L + x \right)} \dot{x}$$

and

$$\dot{P}_2 = \frac{C_f R \sqrt{T}}{V_{02} + A_2 \left(\frac{1}{2} L + x \right)} \left[\alpha_{in} \phi_{in2} \bar{A}_{v2in} P_s \dot{m}_r(P_s, \bar{P}_2) - \alpha_{ex} \phi_{ex2} \bar{A}_{v2ex} \bar{P}_2 \dot{m}_r(\bar{P}_2, P_a) \right] - \alpha \frac{P_2 A_2}{V_{02} + A_2 \left(\frac{1}{2} L + x \right)} \dot{x}$$

Where:

- $R = 8.3144 \text{ L kPa}/(\text{K mol})$ is the ideal gas constant
- Temperature (K) is denoted by T
- α , α_{in} , and α_{ex} take values between 1 and k , however the suitable value for it is $\alpha = 1.2$
- The tube length is denoted by L (m)
- The sound velocity which is 343.2 m/s is denoted by c

- The final pressure is denoted by P (kPa)
- The dynamic viscosity of air is denoted by μ (N/sm²)
- The inner diameter of the tube is denoted by D (m)
- The Reynolds number is denoted by Re (kPa)
- The discharge coefficient is denoted by C_f
- The inactive volume V_{0i}
- The effective piston area denoted by A_i
- The flow function is denoted by m_r
- P_i , $i = 1, 2$ is the absolute pressure in the corresponding cylinder chamber (kPa)
- The source pressure is denoted by P_s (kPa)
- The piston stroke is denoted by L (m)
- The piston position is denoted by x (m)

The movement equation turns out to be the following according to Newton's second law for the cylinder piston:

$$M\ddot{y} = P_1 A_1 - P_2 A_2 - B\dot{y} - F_f - P_{atm} A_{rod}$$

- piston mass is M
- damping coefficient is B
- Friction force is F_f .
- Atmosphere pressure is P_{atm} .
- Cross section is A_{rod} .

2.7 SPOOL VALVE

Some of the type of pneumatic valves that offer versatility in control of the pneumatic equipment are called spool valves. They are also called directional valves based on the configuration. Directional valves are used in pneumatic actuators or motors to control their state. A spool valve has a body which is made of metallic shuttle which has many holes in it. Depending on the valves configuration, it has 3 to 5 ports which are named as inlets, outlets or exhausts respectively.

These holes of the spool are aligned with the valve ports by the use of solenoids which create a flow path through it. The solenoid ensures that the valve is actuated and the spool switches position and is aligned in a proper way to create different flow paths.

Some of the available configurations of spool valves are 3/2, 5/2, 4/3 or 5/3.

These can be categorized according to their functions, such as Solenoid/Spring or Solenoid/Solenoid.

Spool Valves can be made from aluminum, stainless steel, or brass and can be specified for use in numerous Hazardous Area applications.

Directional control valves (DCVs) are one of the most key parts of the actuation system because they allow fluid flow such as hydraulic oil, water or air into different paths. DCVs actuate the spool mechanically or electrically which changes the position and restricts or permits the flow, hence the fluid flow is controlled and this is located inside the cylinder.

2.8 4/3 WAY DIRECTIONAL VALVE

The 4-Way Directional Valve block is given this name because it has four ports and three flow paths. The ports connect to a hydraulic pump (port P), a double-acting actuator (ports A and B), and a storage tank (Port T). Via path P-A or P-B, the fluid flows from the pump to the actuator and from the actuator to the tank via path A-T or B-T.

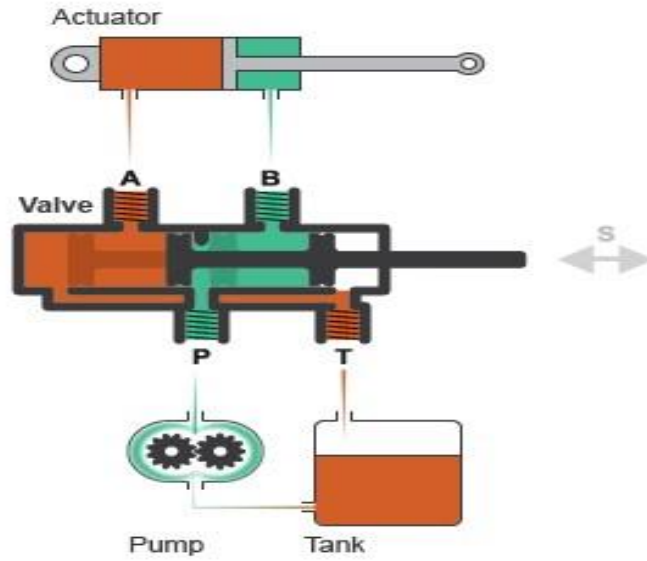


Figure 19: Double Acting Actuator

2.8.1 VALVE CONFIGURATION OF 4/3 DCV

Many other configurations exist. The configuration we are specifically targeting in our discussion are:

Configuration	Initial Openings
	<p>All four orifices are overlapped in neutral position:</p> <ul style="list-style-type: none"> • Orifice P-A initial opening < 0 • Orifice P-B initial opening < 0 • Orifice A-T initial opening < 0 • Orifice B-T initial opening < 0

Figure 20: DCV Configurations

Valve Positions are shown as:

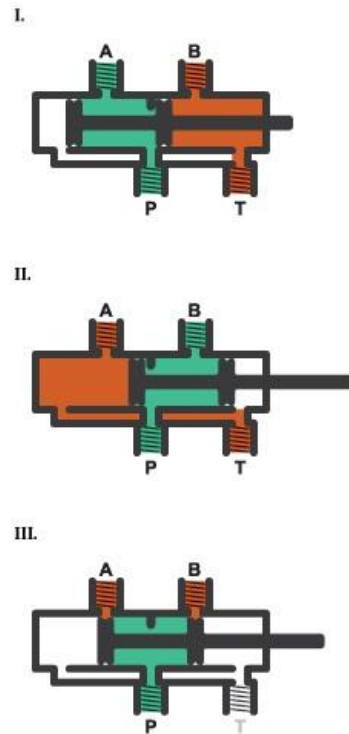


Figure 21: Spool Valve Positions

Port S is called the signal port which controls the spool displacement. The default configuration tells us that the valve position III is the zero displacement signal. A positive signal is given when we want the spool to shift towards the valve position I. Similarly, a negative signal is given when we want the spool to shift towards the valve position II. The spool position is settled relative to each flow path which acts indirectly to the spool displacement. This length is known as the orifice opening. The opening area of the respective flow path is determined by the orifice opening.

2.9 SOLENOID

An electromagnetic device that converts electrical energy into a mechanical push/pull force is called a Linear Solenoid.

Linear solenoid's have a cylindrical tube which has an electrical coil wound around it with a ferro-magnetic actuator which moves in and out of the coil's body. Solenoids can be used to electrically open doors and latches, move and operate robotic limbs and mechanisms, open and close latches, and even actuate electrical switches.

Linear solenoid is one of the common configurations available for solenoids and it is also known as linear electromechanical actuator (LEMA). They are given this name because they move in a straight line. Another type of solenoid that is available is called Rotary Solenoid which produces rotational movement at some angle. These are only some of the few examples of a variety of solenoids available.

The above mentioned solenoids are available in two types which are holding or latching type. Latching type solenoids are used in either energized or power of applications. Linear solenoids can also be designed for proportional motion control in which the plunger position depends on the power input.

When electrical current flows through a conductor it generates a magnetic field around itself. The direction of this magnetic field is determined by the direction of the current flow within the wire. The electric current flowing through the conductor makes it an electromagnet and develops north and south poles similar to a permanent magnet.

We can change the intensity of the magnetic field such as increasing it or decreasing it by the help of changing the current amount to the coil or by changing the number of turns of the coil.

2.9.1 Solenoid Coil's Magnetic Field

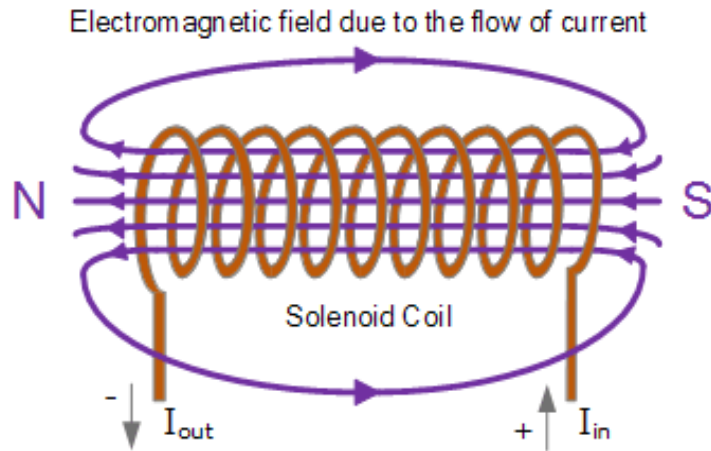


Figure 22: Solenoid Magnetic Field

By passing electricity to the binding we can create an electromagnet which in turn creates a magnetic flux that attracts a plunger which is used to compress the spring. Strength of the magnetic field is directly proportional to the speed and force of the plungers which means that the higher the magnetic field, the higher will be the speed and force of the plunger.

The plunger moves back to its original position due to the energy stored in the compressed spring when the supply current is switched off. Stroke is the name given to this back and forth movement.

- **Construction**

The solenoid in which the plunger moves linearly are called Linear Solenoids.

The linear solenoid that pulls its connected load towards itself is known as Pull-type and the one that pushes it away from itself is known as Push-type when energized. Both of them are designed the same way but with a difference in the location of the return spring and plunger design.

2.9.2 Construction of Pull-Type Solenoid

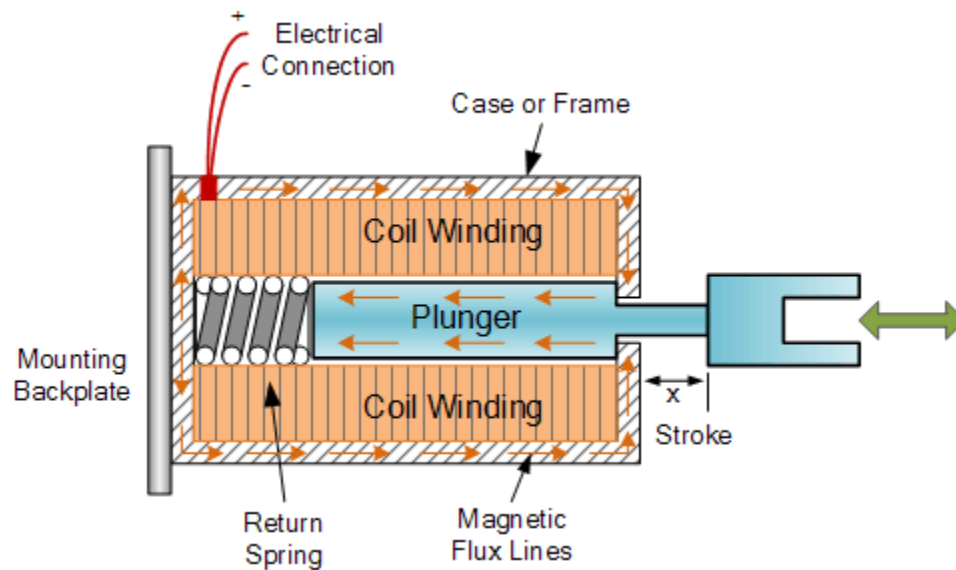


Figure 23: Pull Type Solenoid

For applications such as open or closed type of motion, linear solenoids are used for example in control valves, irrigation valves or engine automation.

2.9.3 Modelling of a Solenoid

The solenoid model consists of an electrical and magnetic circuit which is responsible for the converting input voltage to an electro-magnetic force inside the spool valve. The electrical circuit is the actual coil and has a resistor R in series with a variable inductor L . The control signal determines the voltage given to the solenoid. The voltage–current relationship can be derived as follows:

$$u(t) = L \frac{di(t)}{dt} + i(t)R$$

Where, $u(t)$ is the control voltage, $i(t)$ is the coil current. The pole pieces have been shaped in such a way that it produces a more linear force characteristic and hence the solenoid is termed as proportional. However, linearity can only be maintained for a portion of full solenoid stroke.

The main factors that influence the electro-magnetic force are the current and the displacement of the spool so hence the equation becomes:

$$F_m(t) = f(i(t), x(t))$$

Where $F_m(t)$ is the electro-magnetic force, $x(t)$ is the displacement of the spool. The following equation must be held for each loop in the magnetic circuit, according to Kirchhoff's voltage law:

$$\sum V_{m,n} = \sum \Phi_n \cdot R_{m,n} = 0$$

Where Φ_n is the magnetic flux, $R_{m,n}$ is the magnetic resistance, $V_{m,n}$ is the magnetic voltage.

The statement below is applied to any connection between these components of the magnetic circuit using the definition of magnetic flux:

$$\sum \Phi_i = 0$$

The electric field is given below using the first equation of Maxwell:

$$\oint H \cdot ds = \theta$$

Where H is the magnetic field strength.

The relationship between electric field and magnetic field is

$$V_m = \theta = w \cdot i$$

Where i is the electric current, w is the winding number.

The electric voltage difference V_{Ei} comprises of the voltage drop and the induced voltage in the electromagnetic field.

$$V_{Ei} = R_{Ei} \cdot i + w \cdot \frac{d\Phi}{dt}$$

The electric resistance is denoted by R_{Ei} .

The magnetic field intensity B is according to the following relation:

$$B = \frac{\Phi}{A_a}$$

Where A_a is the area of air gap.

Thus the magnetic field strength is

$$H = \frac{V_m}{l}$$

Where the air gap length is denoted by l .

The magnetic resistance R_m can be stated as

$$R_m = \frac{l}{\mu_0 \cdot A_c}$$

Where the permeability of vacuum is denoted by μ_0 .

The cross-sectional area A_c is

$$A_c = \frac{\pi}{4} \cdot d^2$$

Where the diameter of air gap is denoted by d .

The magnetic voltage is

$$V_m = R_m \cdot \Phi$$
$$H = \frac{B}{\mu_0}$$

Thus, the static magnetic force becomes

Where magnetic flux of air gap is denoted by Φ_{air} .

However, when the spool starts to move with the magnetic force, the air gap length will keep changing. Hence, we get the dynamic magnetic force F_{md} as

$$F_{md} = \frac{1}{2} \cdot \Phi_{Air}^2 \cdot \frac{dR_m}{dl} \quad \text{air} \cdot \frac{l}{\mu_0 \cdot A}$$

2.10 MODELLING OF A VALVE

All the components of the valve model under the effect of electromagnetic and flow forces such as the compression springs, viscous damper and the mass of slide spool. It can be represented by Newton's second law as follows:

$$m \frac{d^2x(t)}{dt^2} + B_v \frac{dx(t)}{dt} + Kx(t) = F_m(t) + F_{st} + F_{tr}$$

K is spring stiffness coefficient, F_{st} and F_{tr} are steady-state flow forces and transient flow forces, m is the spool mass and B_v is the viscous damping coefficient.

2.11 FLOW FORCES

There are two types of flow-induced forces. Steady-state flow forces which are the reaction forces on the spool due to moment of fluid since incompressible flow is assumed. The second type is transient flow forces.

The steady-state flow forces traditional formula is:

$$F_{st} = \rho Q v \cos \theta$$

Q and v is calculated using the following formula:

$$Q = C_d A(x) \sqrt{2\Delta P / \rho}$$

$$V = C_v \sqrt{2\Delta p / \rho}$$

The steady-state flow forces are derived from the above equations:

$$F_{st} = 2C_d C_v A(x) \Delta p \cos \theta$$

Where $\Delta P = P_{in} - P_{out}$, P_{in} and P_{out} are inlet and outlet pressures, C_v is the velocity coefficient, C_d is the discharge coefficient, Q is the flow rate through orifice, ρ is the density of the hydraulic liquid, v is the velocity of the orifice, θ is the flow angle through the orifice, x is the displacement of the spool, and $A(x)$ is the orifice area of the opening position.

The spool has transient flow forces as the reaction forces when the fluid in the annular valve chamber accelerates in response to variation in flow rate. The transient flow has the following formula:

$$F_{tr} = -\rho l \frac{d}{dt} Q = C_d l \sqrt{2\rho \Delta P} \frac{dA(x)}{dt}$$

In which, l is the length of the fluid columns and $A(x)$ is the orifice area.

2.11.1 ORIFICE AREA

The cross section of an orifice with variable round holes is shown using the following formula:

$$A(x) = \begin{cases} d^2(\theta - \sin \theta)/8, & x_{max} \geq x > U \\ 0, & 0 < x \leq U \end{cases}$$

In which,

$$\theta = 2 \arccos(1 - (2x - U)/d)$$

Here, the hole diameter of the orifice is denoted by d , the orifice initial opening is denoted by U , and x is the spool displacement from initial position.

Solenoid current and the displacement forces are given as:

$$F_m(t) = K_f(x_e) i(t)$$

The equation of steady-state and transient flow forces become as follows due to Taylor Series Expansion:

$$F_{st} = 2C_d C_v A(x) \Delta P \cos \theta = B_s(x_e)x$$

$$F_{tr} = C_d \sqrt{2\rho \Delta P} \frac{dA(x)}{dt} = B_t(x_e) \frac{dx}{dt}$$

Here B_t is damping coefficient of the transient flow forces, B_s is stiffness of steady-state flow forces,

The transfer functions are derived for Coil current transfer function using Laplace transformation:

$$I(s) = \frac{U(s)}{Ls + R}$$

Electro-magnetic transfer function is given as:

$$F_m(s) = K_f(x_e)I$$

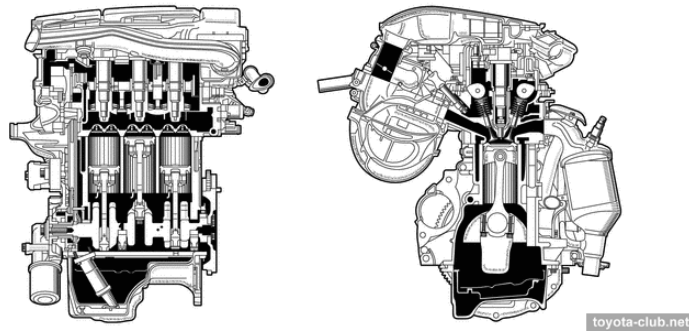
Valve transfer function is given as:

$$X(s) = \frac{F_m(s)}{ms^2 + (B_v(x_e) + B_t(x_e))s + (K + B_s)}$$

CHAPTER 3 : METHODOLOGY

3.1 ACQUIRING ENGINE DATA

To produce the proposed system, it was essential to choose an engine according to which the system would be designed. Toyota's 1KR-FE engine was selected, usually fitted inside Toyota's smaller car variants such as the Passo or Daihatsu's Boon, as all the required data was available. The engine data is as follows:



Engine Manufacturer	Toyota 1KR-FE
Engine Type	4 Stroke Spark Ignition
Fuel Type	Petrol
Charge System	Naturally Aspirated
Valves per cylinder	2
Displacement	996cm ³
Cylinder Alignment	In Line 3
Max RPM	6000
Bore	71mm
Stroke	83.9mm
Compression ratio	12.5:1
Net Horse Power	68hp
Net Torque	92Nm

Table 1: 1KR-FE Engine Data

3.2 SVAJ DIAGRAMS

For any system, it is critical to define bounding values to what a system can realistically achieve. As the system revolves around designing an alternate valve actuation system to the conventional cam shaft and cam-follower mechanism, it was important to use cam analysis to generate values for displacement, velocity, acceleration and jerk.

$$\text{Given: } s = f(t) \quad \{\text{displacement or position}\}$$

$$v = \frac{ds}{dt} = f'(t) \quad \{\text{velocity}\}$$

$$a = \frac{dv}{dt} = f''(t) = \frac{d^2s}{dt^2} \quad \{\text{acceleration}\}$$

$$j = \frac{da}{dt} = f'''(t) = \frac{d^3s}{dt^3} \quad \{\text{jerk}\}$$

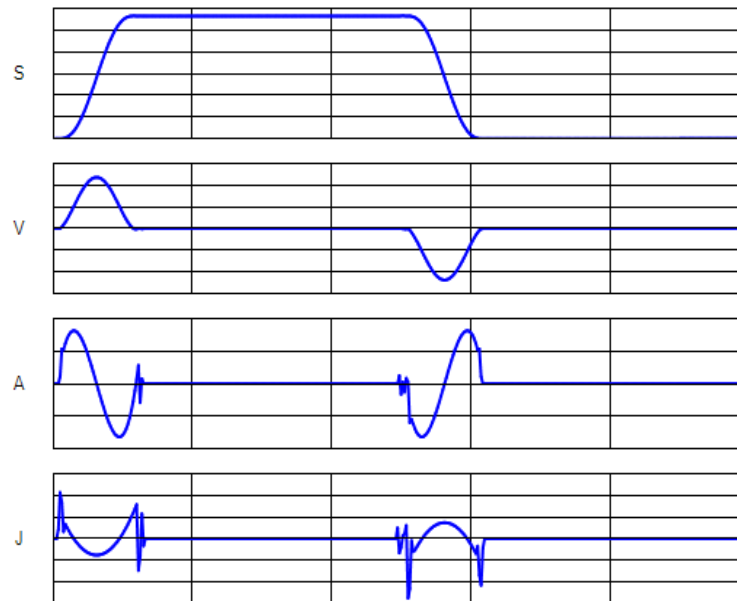


Figure 24: SVAJ Plots for 800 RPM

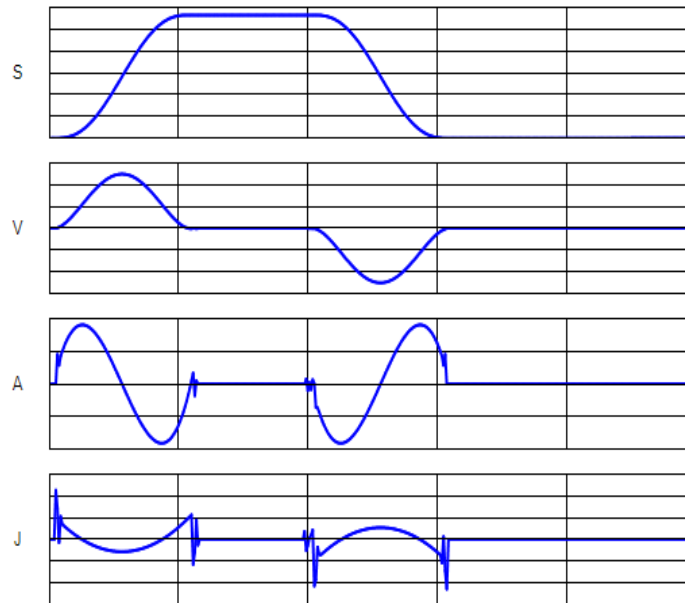


Figure 25: SVAJ Plots for 4000RPM

The analysis would produce finite values for displacement, velocity, acceleration and jerk, which will be used as a reference to generate feasible valve displacement graphs for the valve actuation system.

Discussing the graphs for the two extreme analysis RPM values, it is evident that the duration of peak lift is significantly greater for 800RPM as compared to 4000RPM. Consequently as velocity, acceleration and jerk are derived values from displacement, and they vary accordingly. It is important to acknowledge that the plotted variables are generated to produce finite values for the system as evident from the diagrams.

3.3 VALVE TRAIN DYNAMICS

After bounding values for the valve displacement have been defined used cam analysis, valve displacement diagrams were generated using curve fitting tool in MATLAB and hence a set of values was attained with respect to CAD to define the motion of the valve.

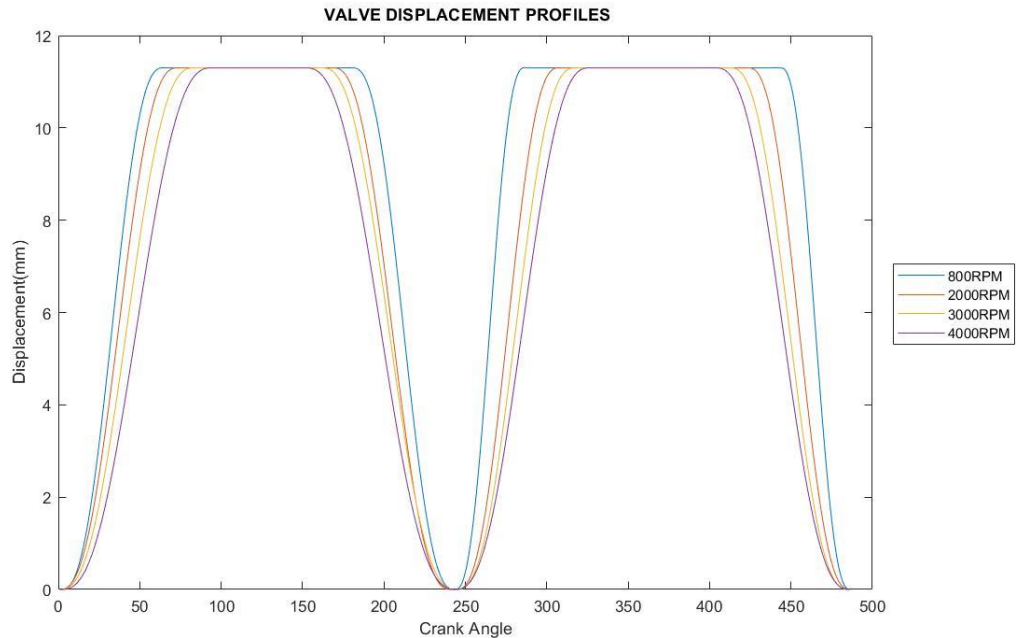


Figure 26: Valve Displacement Plots

This plot showcases the motion followed by both intake valve (right plot) and exhaust valve (left plot). Some characteristics of the diagram are:

- Intake Valve has a longer duration of peak lift for all RPMs as compared to exhaust valve, to accommodate for relatively slower air flowing into the cylinder than flowing out of the cylinder.
- For each valve, duration of peak lift decreases with RPM and hence producing a less steep rise and fall curve. This ultimately gives us reasonable values for forces acting on the valve to be supplied by the valve actuation system.
- Peak lift value is set at 11.3mm, which is approximately 15% of bore size. This can be reduced or increased as per engine requirements, fulfilling the VVL aspect of the system.
- The duration of peak lift can be varied to fulfill the VVD aspect of the system.
- The displacement plots can be shifted forward or backward (cam phasing) to accommodate valve overlap. This fulfills the VVT aspect of the system.

RPM/Stroke	Rise	Return
800RPM	$2.6418x^5 + 2.5197e^{-13}x^4 - 8.0817x^3 - 4.6159e^{-08}x^2 + 11.092x + 5.65$	$-1.527e^{-08}x^5 + 1.565e^{-5}x^4 - 0.006324x^3 + 1.259x^2 - 123.4x + 4790$
2000RPM	$2.854e^{-08}x^5 - 5.77e^{-06}x^3 + 0.0003223x^3 - 0.002146x^2 + 0.003694x - 0.0007526$	$-2.854e^{-08}x^5 + 2.996e^{-05}x^4 - 0.01245x^3 + 2.558x^2 - 260x + 1.048e^{-04}$
3000RPM	$5.834e^{-08}x^5 - 1.021e^{-05}x^4 + 0.0005082x^3 - 0.003329x^2 + 0.005678x - 0.001109$	$5.834e^{-08}x^5 + 6.272e^{-05}x^4 - 0.02676x^3 + 5.665x^2 - 595x + 2.483e^{-04}$
4000RPM	$3.602e^{-07}x^5 - 4.578e^{-05}x^4 + 0.001664x^3 - 0.001035x^2 + 0.01714x - 0.003184$	$-3.662e^{-07}x^5 + 0.000412x^4 - 0.11848x^3 + 41.29x^2 - 4598x + 2.042e^{-05}$

Table 2: Valve displacement functions

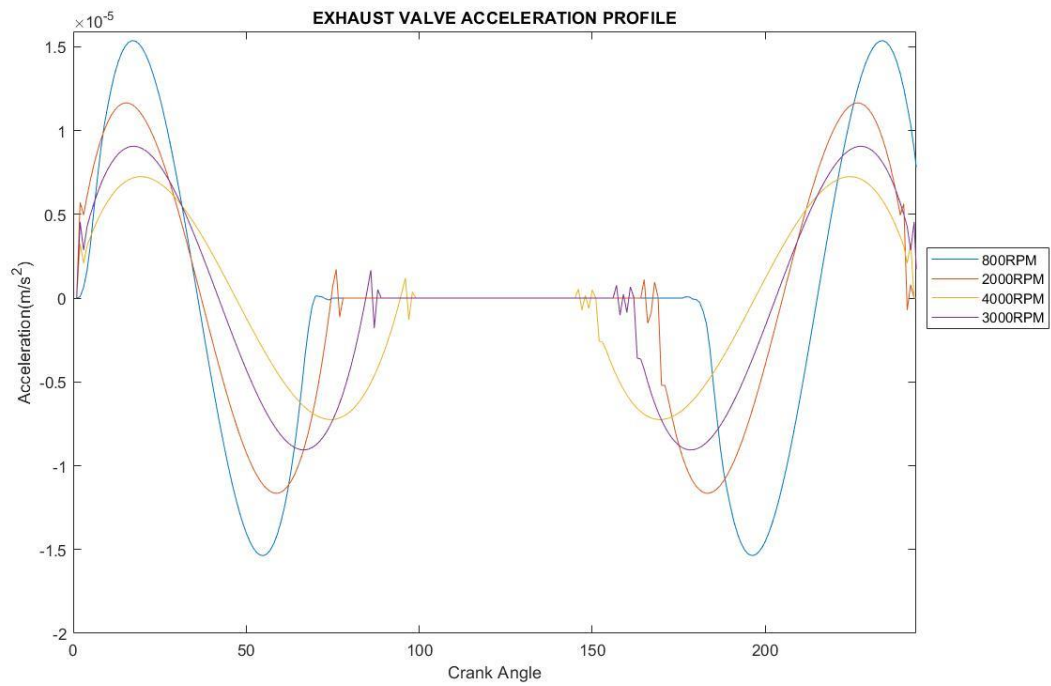


Figure 27: Valve Velocity Profiles

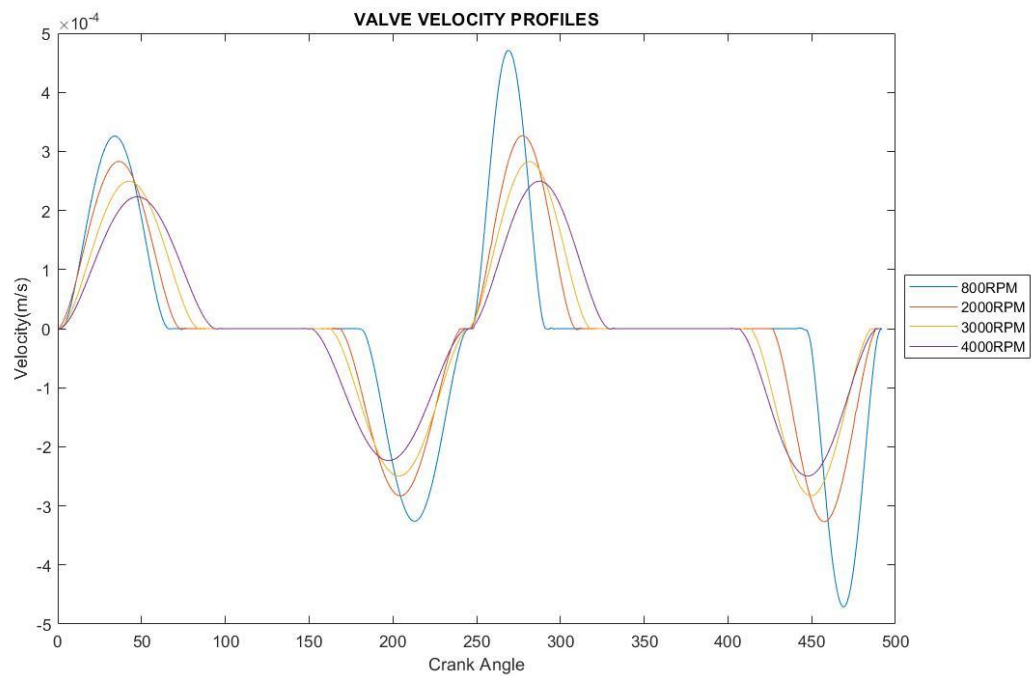


Figure 28: Valve Acceleration Profiles

3.4 DESIGN

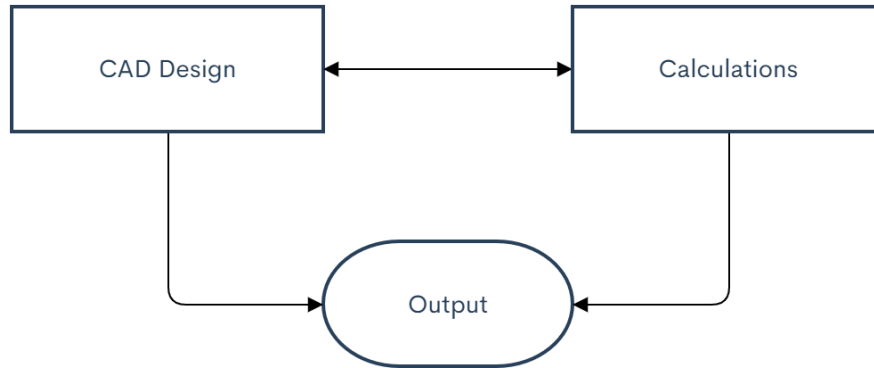


Figure 29: Design Mental Map

Once the required output of the system is generated, system is designed to ensure the output is achieved. Using trial and error, a CAD design was finalized which had realistic working conditions for the chosen engine. The final design is as follows:

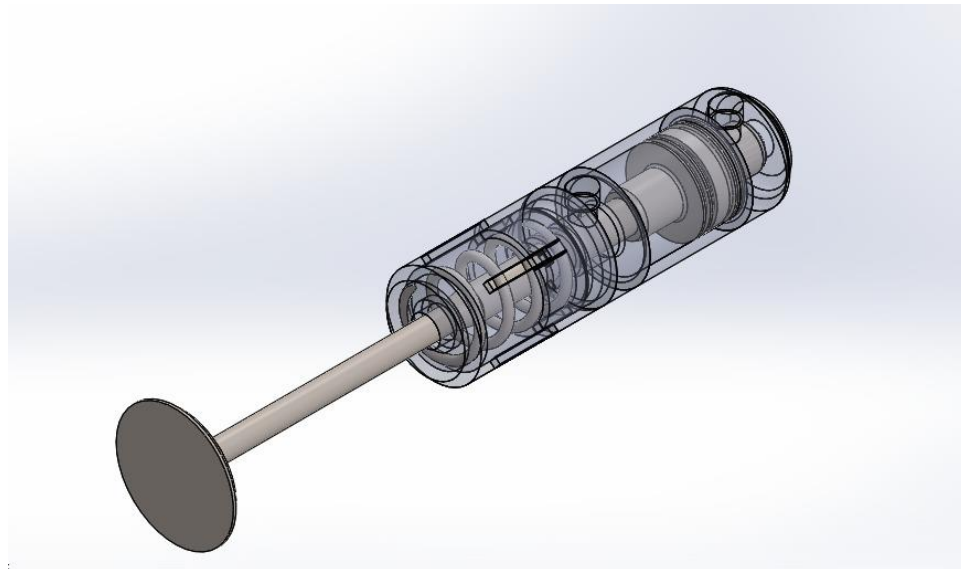


Figure 30: Proposed DAPA Design

Figure 30 shows the designed pneumatic actuator. The main characteristics of the actuator are:

- It is a double acting pneumatic actuator (DAPA)
- Includes a return spring to aid return stroke
- Spring is enclosed in a housing with an internal holder to prevent buckling
- Consists of a pressure chamber with inlet ports on either side of the plunger
- Plunger end acts as a cushioning piston to reduce impact force by providing a hard stop damping force.
- Engine Valve attached directly to plunger, size is as specified for the chosen engine
- Excess flow valves incorporated to release excess pressure if needed
- Chamfers added to reduce stress concentrations.

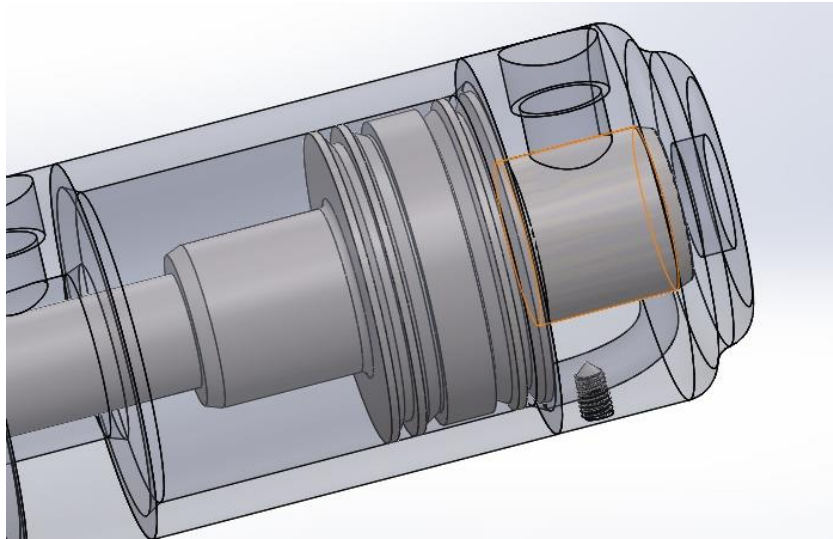


Figure 31: Pressure Chamber with Excess Flow Valve

Each valve has its own actuator. A housing is manufactured and fitted above the engine block as shown in Figure 10, accommodating all actuators, pipe systems and coolant channels.

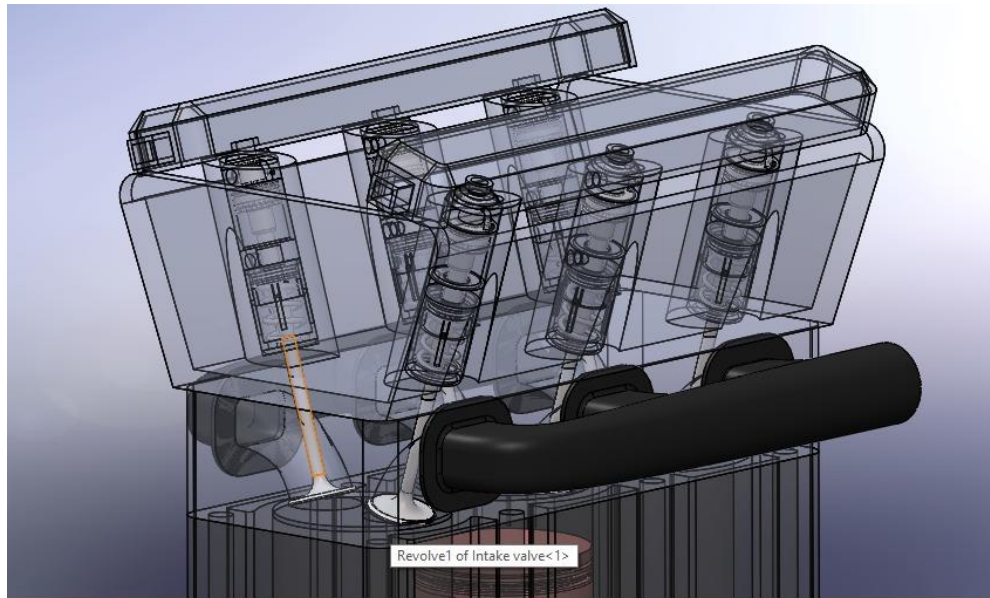


Figure 32: Actuator Housing

After finalizing the design, dimensions of different components were decided on considering system requirements and limitations. Following that would be selecting suitable materials that would be able to withstand the working conditions and provide robustness and reliability.

The materials chosen were:

- **Stainless Steel Grade 304**

Stainless Steel grade 304 is usually use to manufacture pressure vessels as they are extremely resistant to chemicals, and provide high corrosion resistance. It has the capability of withstanding humid conditions and high temperatures.

- **Inconel 751**

INCONEL alloy 751 is normally used to manufacture valve in internal-combustion engines. The alloy offers high operating strength at higher temperatures, good wear resistance, and corrosion resistance which in contact with hot cylinder mixtures containing lead oxide, sulfur, bromine, and chlorine.

- **Aluminum Alloy**

These materials possess high strength, high corrosion resistance, low density, lower thermal expansion coefficients, and good castability and provide good vibration resistance.

Usually used as an alternative to cast iron for engine block manufacture.

- **Hard Drawn MB ASTM A227**

Component	Material
Valve	Inconel 751
Spring Housing	Stainless Steel 304
Spring	Hard Drawn MB ASTM A227
Pressure Chamber	Stainless Steel 304
Plunger Assembly	Stainless Steel 304
Actuator Housing	Aluminum Alloy

Table 3: Component Materials

Component	Material	Mass/g
Pressure Chamber	Stainless Steel 304	85.63
Plunger	Stainless Steel 304	45.58
Spring Housing	Stainless Steel 304	42.46
Spring	Hard Drawn MB ASTM A227	4.33
Valve	Inconel 625	20.45
Actuator Assembly		198.48

Table 4: Component Masses

3.5 SIMULATION AND SIMULINK ANALYSIS

The underlying goal of the project was to validate the theoretical calculations and support them with relevant simulations. A realistic model of the pneumatic actuation system is necessary to understand the design and make sure it is functional in the given scenario. Since, there was no data acquisition software or experimental setup to accumulate the real-life data, theoretical calculations for valve train dynamics were done on MATLAB and Microsoft Excel. This data was used to run simulations on SIMULINK. A pneumatic actuation circuit was created on SIMULINK to produce the desired output by setting working conditions and design parameters.

The model shown in Figure 11 includes:

A Translational Mechanical Converter to simulate a Double acting pneumatic actuator (DAPA)

A 4/3 directional control valve (DCV) to control the flow of air in and out of the DAPA,

- A pipe network that supports the circuit by flowing air from reservoir up to the double acting cylinder and then back to the reservoir in backward stroke.
- An electro-mechanical solenoid to provide a specific spool input to the 4/3 DCV.
- The 4/3 directional control valve is used as per our specific need. The 4/3 directional control valve is controlled using spool.
- Position sensors to plot displacement profile followed by spool and actuator.

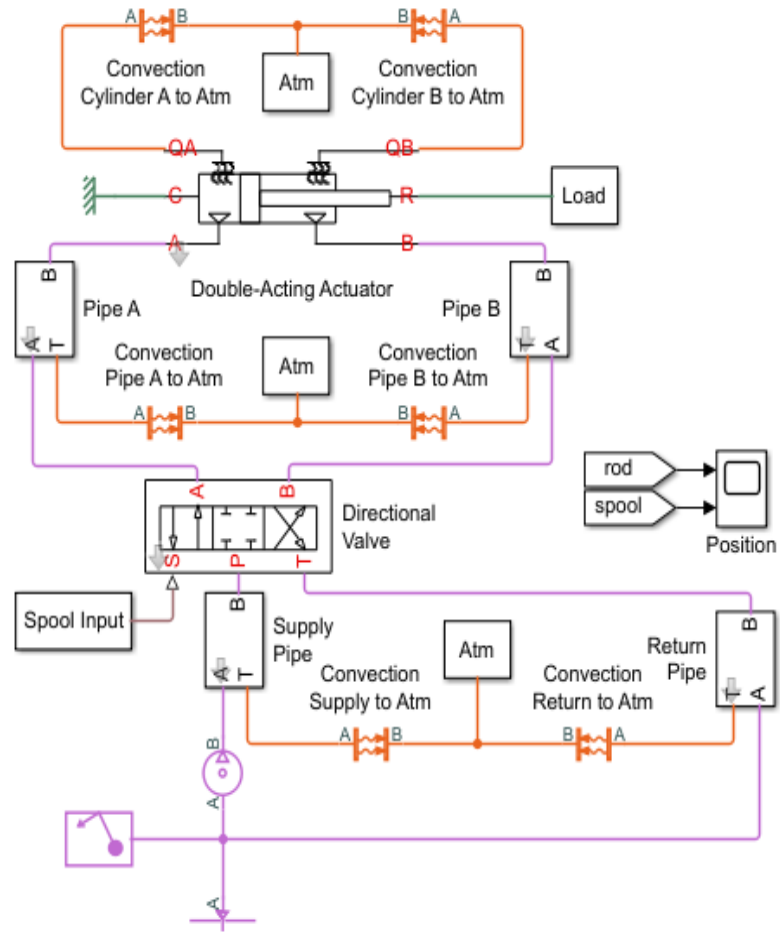


Figure 33: Pneumatic Circuit Schematic

The basic working of the circuit shown in Figure 11 above is that spool input of the DCV oscillates between the maximum positive and negative displacement positions, enabling compressed air to flow from the reservoir into the actuator chamber and controls the stroke of the pneumatic actuator as required. The simulation takes into account the thermal properties of the components and effect of surrounding thermal conditions into the motion of the actuator piston.

Figure 34 shown below shows the directional control valve (DCV) subsystem.

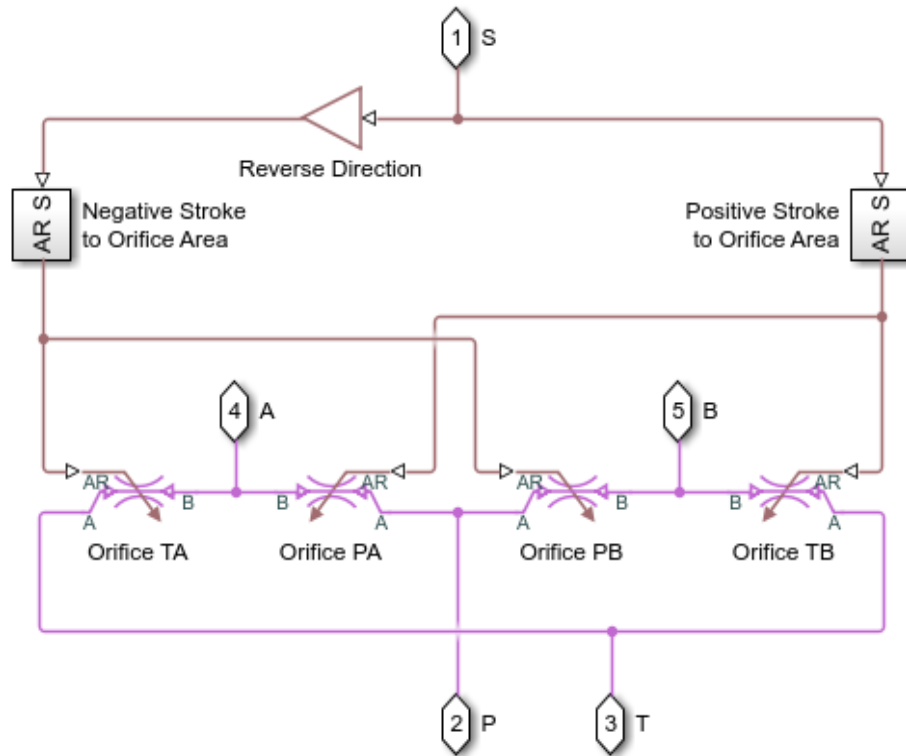


Figure 34: DCV Subsystem

Orifice PA and Orifice TB open when the DCV Spool position is positive. It allows fluid to flow from port P to port A and from port B to port T. When the valve spool position is negative, air flows flow from port P to port B and from port A to port T. The double acting actuator is subject to a fixed load for every RPM equivalent to values calculated using valve train dynamics concepts.

The double acting actuator subsystem shown in Figure 13 shows two translational converters for lift and return strokes.

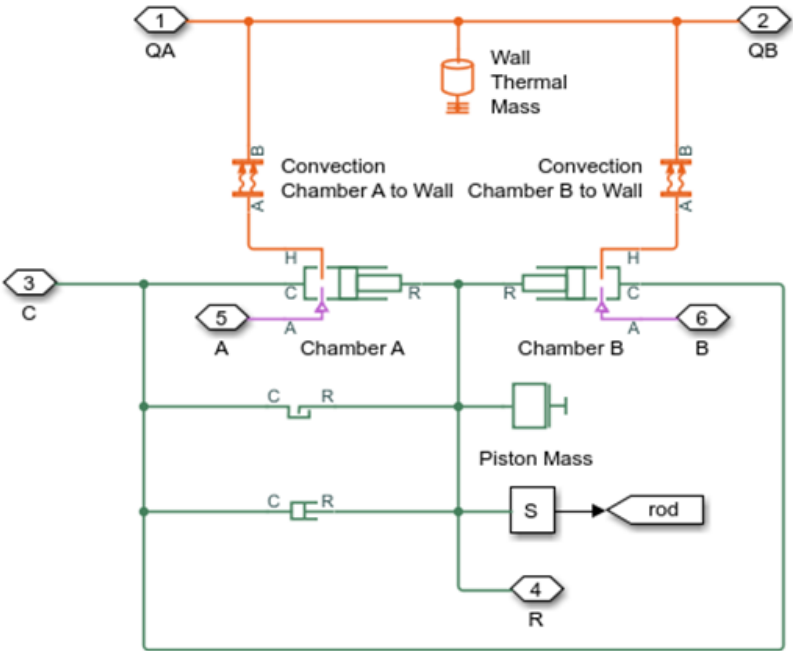


Figure 35: DAPA Subsystem

The double acting actuator subsystem shown in Figure 13 shows two translational converters for lift and return strokes.

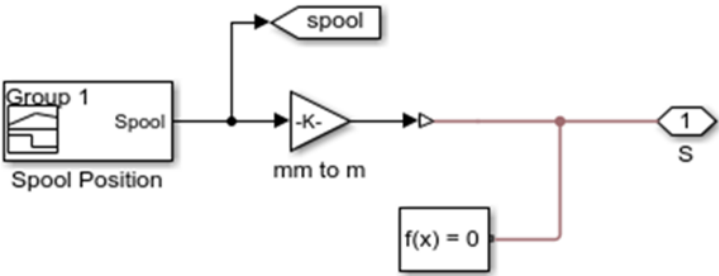


Figure 36: Spool Input Subsystem

The Spool input subsystem shown in figure 3.11 provides the electrical control input to the DCV which subsequently controls DAPA motion.

The gas properties of the air that is flowing across circuit depending on the crankshaft RPM are given in Table 5 below.

		RPM			
Property/RPM	Units	800	2000	3000	4000
Gas Specification		Perfect	Perfect	Perfect	Perfect
Specific gas constant	kJ/kg/K	0.287	0.287	0.287	0.287
Compressibility Factor		1	1	1	1
Reference Temperature	K	298.15	323.15	343.15	368.15
Reference Enthalpy	kJ/kg	298.15	323.34	343.68	368.43
Specific Heat Capacity(Constant Pressure)	kJ/kg/K	1.007	1.007	1.007	1.008
Dynamic Viscosity	s.μPa	18.49	19.63	20.52	21.64
Thermal Conductivity	mW/m/K	25.59	27.35	28.81	30.60

Table 5: Gas Properties

Piston Area	0.00070695	m ²
Connection Port Area	5e-06	m ²
Maximum Stroke	11.63	Mm
Mechanical Damping	200	N/m*s
Hard Stop Stiffness	1e07	N/m
Hard stop Damping	1500	N/m*s
Piston Mass	g	66.03
Actuator Total Mass	g	198.48

Table 6: DAPA Data

Discharge Coefficient	0.82	
Maximum Orifice Area	4e-06	m ²
Displacement Limit	5e-03	m
Leakage area	1e-10	m ²
Displacement for Leakage area	2e-04	m
Connection port area	5e-06	m ²

Table 7: DCV Working Parameters

Piping Cross-sectional area	5e-06	m ²
Pipe wall density	1500	Kg/m ³
Pipe wall specific heat	1250	kJ/kg.K
Ambient Pressure	0.1013	MPa
Maximum Pressure Differential	0.8	MPa
Convection supply area		m ²
Convective Heat transfer coefficient	20	W/(m ²).K
Pressure Source port area	5e-06	m ²

Table 8: Pneumatic Circuit Working Conditions

3.6 SOLENOID AND DCV SELECTION

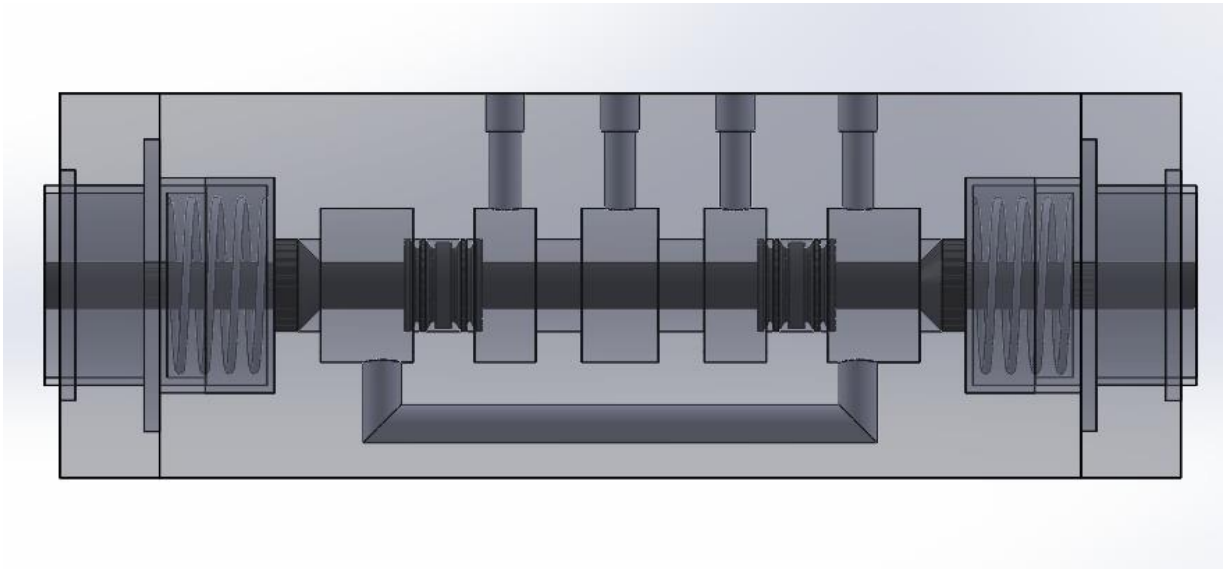


Figure 37: DCV with double solenoid control

As mentioned above, the pneumatic circuit consists of a 4/3 Directional control valve. 4/3 stands for 4 connection ports and 3 spool positions. The spool position is controlled by a solenoid that provides a force at appropriate intervals to actuate the system.

The DCV used in this system will incorporate two linear, push-type control solenoids with return springs. This is to halve the operating frequency at any given RPM. The spool piston was designed with appropriate materials and dimensions to minimize mass and hence reduce dynamic forces. After acquiring appropriate spool position data from the simulations, properties of the solenoid and spring were set to generate required forces and simultaneously using less power.

The spool piston mass was kept as small as possible to minimize dynamic forces and hence reducing load on the solenoid.

Spool Position varies as RPM increases as the simulations suggest. Due to different system requirements as different RPMs, it is important to analyze feasibility of each state.

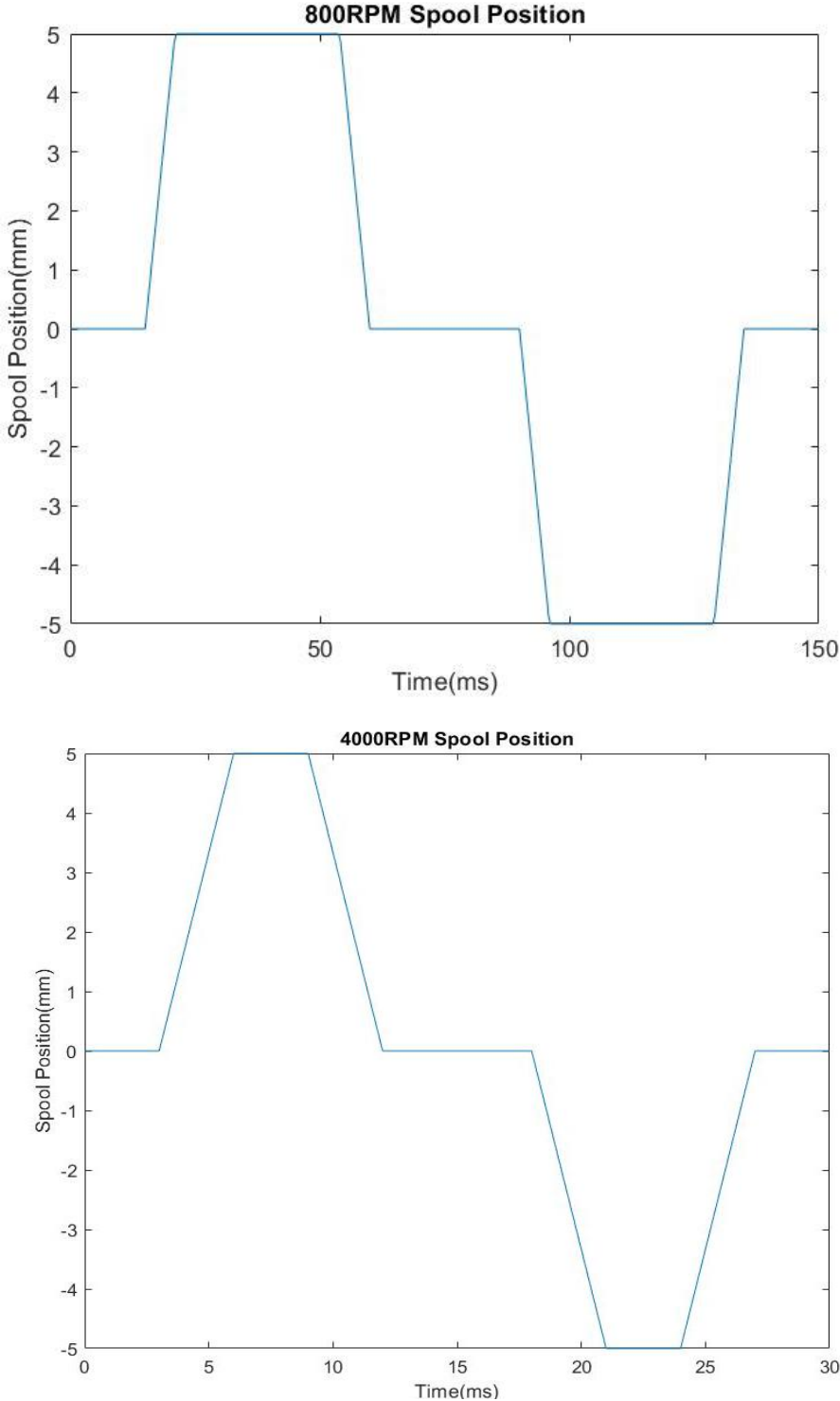


Figure 38: Spool Positions for different RPMS

Solenoid Property	RPM			
	800RPM	2000RPM	3000RPM	4000RPM
Average Force(N)	4.00	5.31	5.98	6.81
Frequency(Hz)	6.6667	16.6667	25	33.3333

Table 9: Solenoid Data

3.7 STRUCTURAL ANALYSIS

The actuator is subject to different types of loadings during its life cycle. It is important to manufacture a reliable system with robust components, able to withstand deformation without failure.

Structural analysis was done on Ansys Mechanical, using the pre-made CAD design.

Mesh was generated with a suitably small element size that would give accurate results but also would reduce computation time.

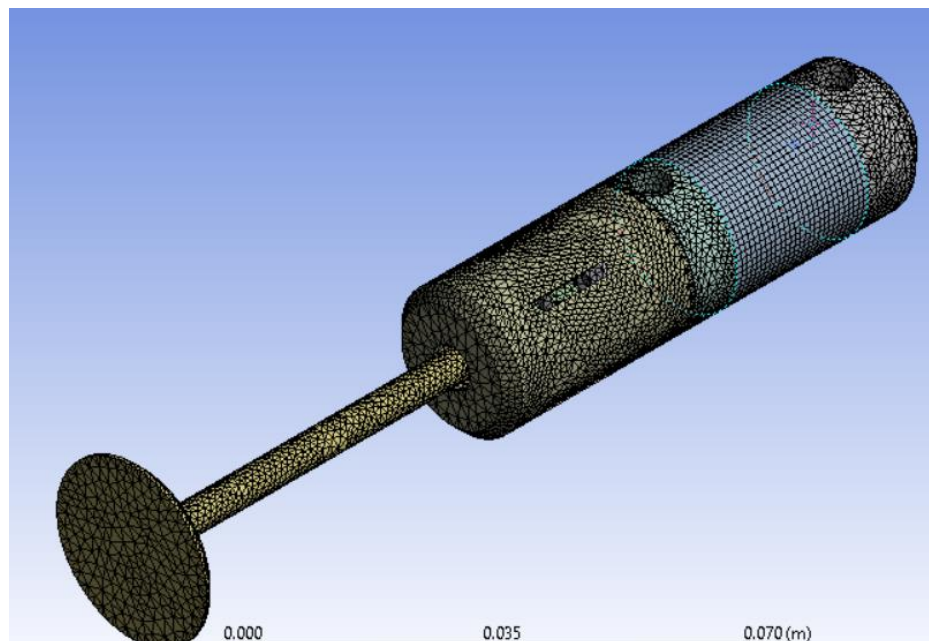


Figure 39: Generated Mesh for Analysis

Forces applied included:

- Axial Forces, to accommodate dynamic loads
- Pressure force due to compressed air entering chamber
- Thermal stresses

As the loadings are cyclic, fatigue loadings are also applied and cycles to failure were also generated. Goodman's Theory of failure used to compute cycles to failure.

3.8 CFD ANALYSIS

A simplified 2D model was created and simulated on ANSYS Fluent to verify and observe the velocity profiles generated. The flow has been assumed to be steady, incompressible and 2 dimensional. The values of Static Pressure, air Velocity were incorporated in the solver. The SST k-omega model has been used to model turbulence (Huang & GAO, 2012).

The model was designed using original CAD design specifications. Simplistic design was used instead of 3D model to avoid complexity and ensuring better results.

In this 2D simulation, air flows through the inlet orifice into the actuator and pushes the piston forward. Dynamic meshing was generated and implemented to simulate piston movement due to flow into the chamber.

The dynamic mesh was done using the layering method. A profile file was implemented as cell zone condition and used in dynamic meshing for the piston wall. The profile file was created for displacement against time with data acquired from the theoretical calculations. Meshing was done in accordance with dynamic meshing calculations. Face meshing was implemented with controlled element size (0.0001m) so that we have precise solutions.

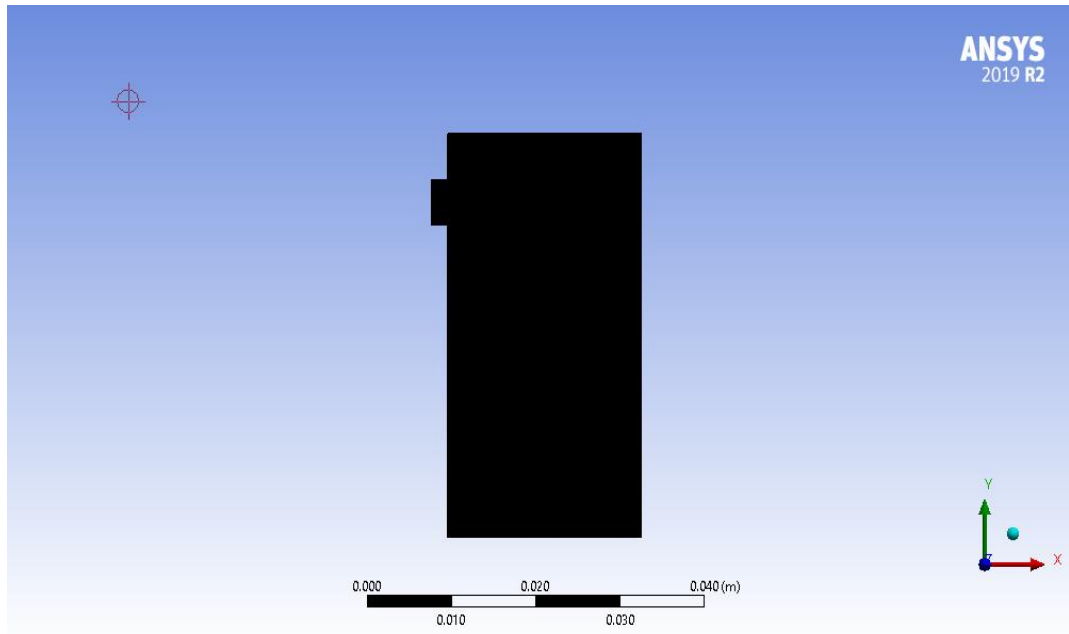


Figure 40: Generated Mesh for 2D Structure

The continuity and momentum equations for the problem are as follows;

Continuity:
$$\frac{\partial \rho}{\partial t} + \frac{\partial(\rho u)}{\partial x} + \frac{\partial(\rho v)}{\partial y} + \frac{\partial(\rho w)}{\partial z} = 0$$

X – Momentum:
$$\frac{\partial(\rho u)}{\partial t} + \frac{\partial(\rho u^2)}{\partial x} + \frac{\partial(\rho uv)}{\partial y} + \frac{\partial(\rho uw)}{\partial z} = -\frac{\partial p}{\partial x} + \frac{1}{Re_r} \left[\frac{\partial \tau_{xx}}{\partial x} + \frac{\partial \tau_{xy}}{\partial y} + \frac{\partial \tau_{xz}}{\partial z} \right]$$

Y – Momentum:
$$\frac{\partial(\rho v)}{\partial t} + \frac{\partial(\rho uv)}{\partial x} + \frac{\partial(\rho v^2)}{\partial y} + \frac{\partial(\rho vw)}{\partial z} = -\frac{\partial p}{\partial y} + \frac{1}{Re_r} \left[\frac{\partial \tau_{xy}}{\partial x} + \frac{\partial \tau_{yy}}{\partial y} + \frac{\partial \tau_{yz}}{\partial z} \right]$$

Z – Momentum:
$$\frac{\partial(\rho w)}{\partial t} + \frac{\partial(\rho uw)}{\partial x} + \frac{\partial(\rho vw)}{\partial y} + \frac{\partial(\rho w^2)}{\partial z} = -\frac{\partial p}{\partial z} + \frac{1}{Re_r} \left[\frac{\partial \tau_{xz}}{\partial x} + \frac{\partial \tau_{yz}}{\partial y} + \frac{\partial \tau_{zz}}{\partial z} \right]$$

Energy:
$$\frac{\partial(E_T)}{\partial t} + \frac{\partial(uE_T)}{\partial x} + \frac{\partial(vE_T)}{\partial y} + \frac{\partial(wE_T)}{\partial z} = -\frac{\partial(up)}{\partial x} - \frac{\partial(vp)}{\partial y} - \frac{\partial(wp)}{\partial z} - \frac{1}{Re_r Pr_r} \left[\frac{\partial q_x}{\partial x} + \frac{\partial q_y}{\partial y} + \frac{\partial q_z}{\partial z} \right] + \frac{1}{Re_r} \left[\frac{\partial}{\partial x} (u \tau_{xx} + v \tau_{xy} + w \tau_{xz}) + \frac{\partial}{\partial y} (u \tau_{xy} + v \tau_{yy} + w \tau_{yz}) + \frac{\partial}{\partial z} (u \tau_{xz} + v \tau_{yz} + w \tau_{zz}) \right]$$

The inlet boundary type is chosen as inlet velocity and turbulence intensity as these parameters can be calculated using the theoretical formulas.

The above continuity and momentum equations are solved iteratively using the given boundary conditions, the CFD solver till the error between two successive iterations is less than a specified value.

The calculations were done for time step size of 0.025 with 200 time steps. 50 calculations per time step were implemented for precise calculations.

Once the iterations are done, results for velocity and pressure are generated.

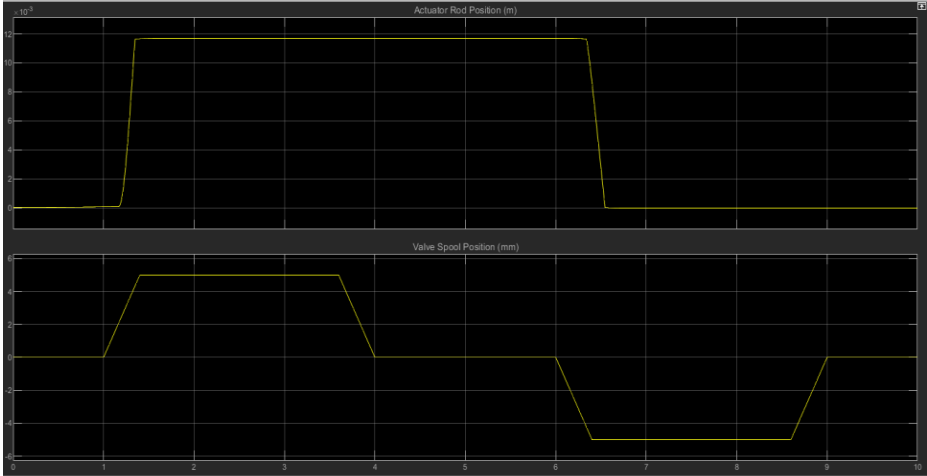
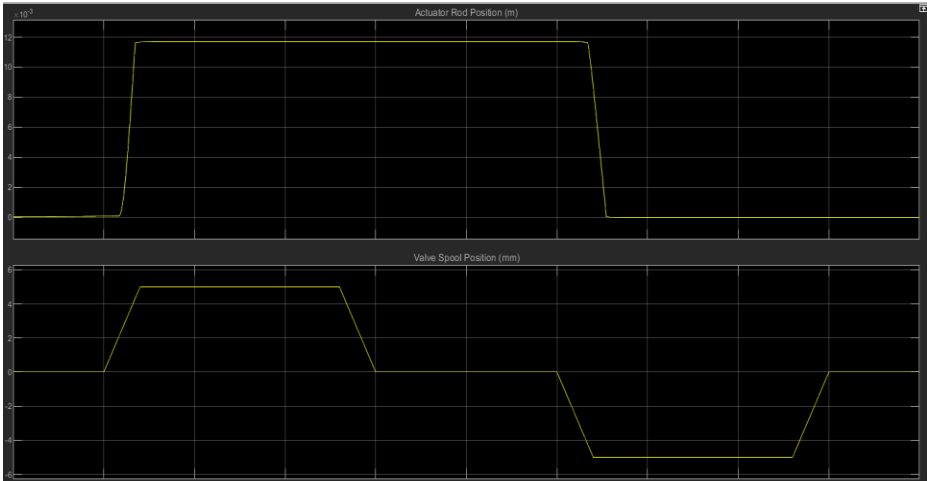
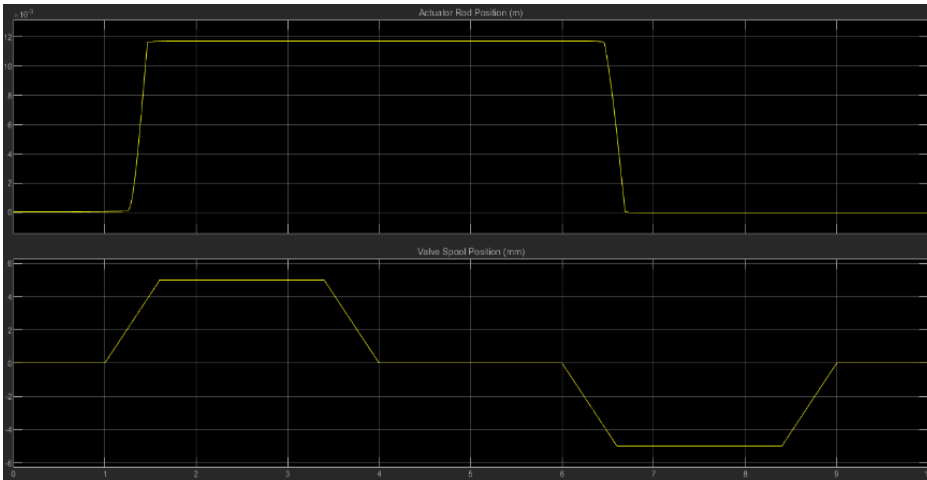
Parameter	Inlet Velocity [m/s]	Inlet Gauge Pressure [MPa]
800 rpm	174	1.01325
2000 rpm	192	1.01325
3000 rpm	228	1.01325
4000 rpm	264	1.01325

Table 10: Inlet Fluid Flow Conditions

CHAPTER 4 : RESULTS

4.1. PARAMETRIC AND GRAPHIC RESULTS

Parameter	units	RPM			
		800	2000	3000	4000
Peak Lift	mm	11.3	11.3	11.3	11.3
Peak Velocity	mm/s	0.000471177	0.0000326695	0.0002829777	0.00024952
Peak Acceleration	m/s ²	3.1637E-05	1.74166E-05	1.16455E-05	9.0565E-06
Peak Force	N	77.265	265.84761	399.475021	544.427034
Peak Jerk	mm/s ³	5.92E-06	5.71E-06	5.62945E-06	4.26384E-06
Maximum Chamber Pressure	MPa	0.7	0.7	0.7	0.7
Maximum Mass Flow Rate(though DCV)	Kg/s	3.6E-04	3.2E-04	2.98E-04	2.42E-04
Maximum Chamber Temperature	C	365	365	365	365
Chamber Inlet Velocity	m/s	174	192	228	264
Inlet Mach	-	0.522	0.5765	0.6846	0.79279
Reservoir Pressure	MPa	0.8	0.8	0.8	0.8

RPM	Parameter	Graphical Results
800	Lift Spool Position	 <p>The graph for 800 RPM consists of two vertically stacked plots. The top plot, titled 'Actuator Rod Position (m)', shows a signal that starts at 0, rises to approximately 10 (scaled by 10^{-3}) at time 1, remains constant until time 6, and then falls back to 0. The bottom plot, titled 'Valve Spool Position (mm)', shows a signal that starts at 0, rises to approximately 4 at time 1, remains constant until time 4, falls to approximately -4 at time 6, remains constant until time 8, and then rises back to 0.</p>
2000	Lift Spool Position	 <p>The graph for 2000 RPM consists of two vertically stacked plots. The top plot, titled 'Actuator Rod Position (m)', shows a signal that starts at 0, rises to approximately 10 (scaled by 10^{-3}) at time 1, remains constant until time 6, and then falls back to 0. The bottom plot, titled 'Valve Spool Position (mm)', shows a signal that starts at 0, rises to approximately 4 at time 1, remains constant until time 4, falls to approximately -4 at time 6, remains constant until time 8, and then rises back to 0.</p>
3000	Lift Spool Position	 <p>The graph for 3000 RPM consists of two vertically stacked plots. The top plot, titled 'Actuator Rod Position (m)', shows a signal that starts at 0, rises to approximately 10 (scaled by 10^{-3}) at time 1, remains constant until time 6, and then falls back to 0. The bottom plot, titled 'Valve Spool Position (mm)', shows a signal that starts at 0, rises to approximately 4 at time 1, remains constant until time 4, falls to approximately -4 at time 6, remains constant until time 8, and then rises back to 0.</p>

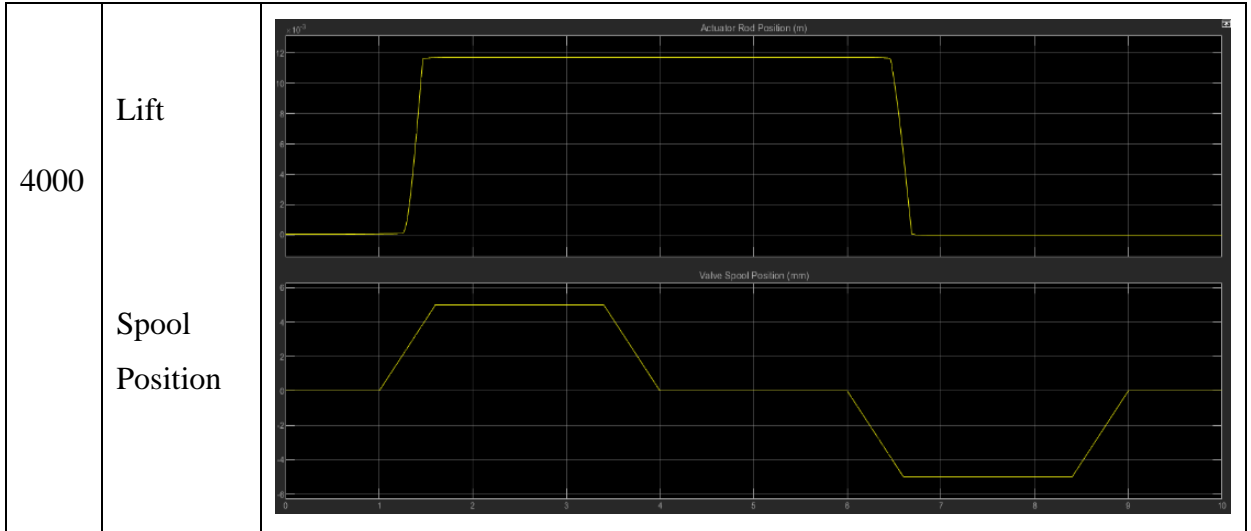
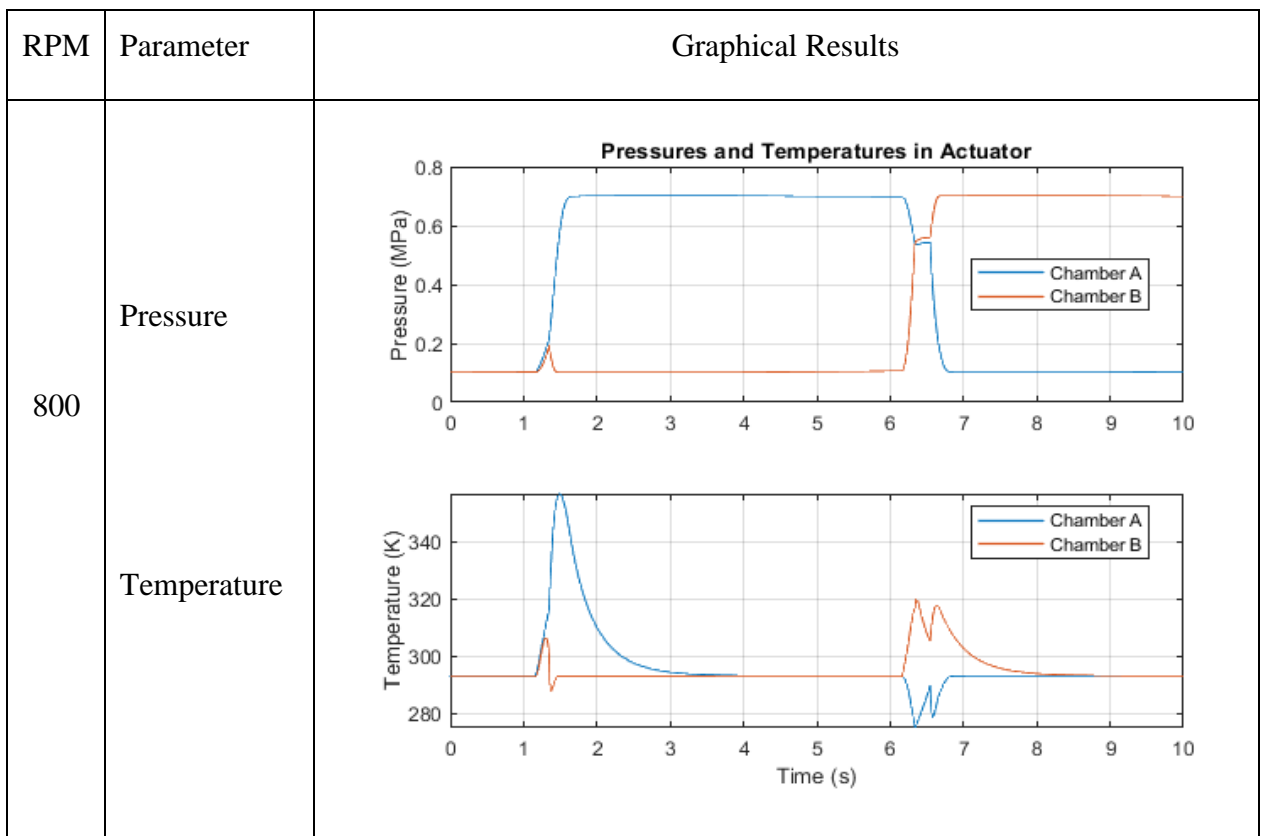
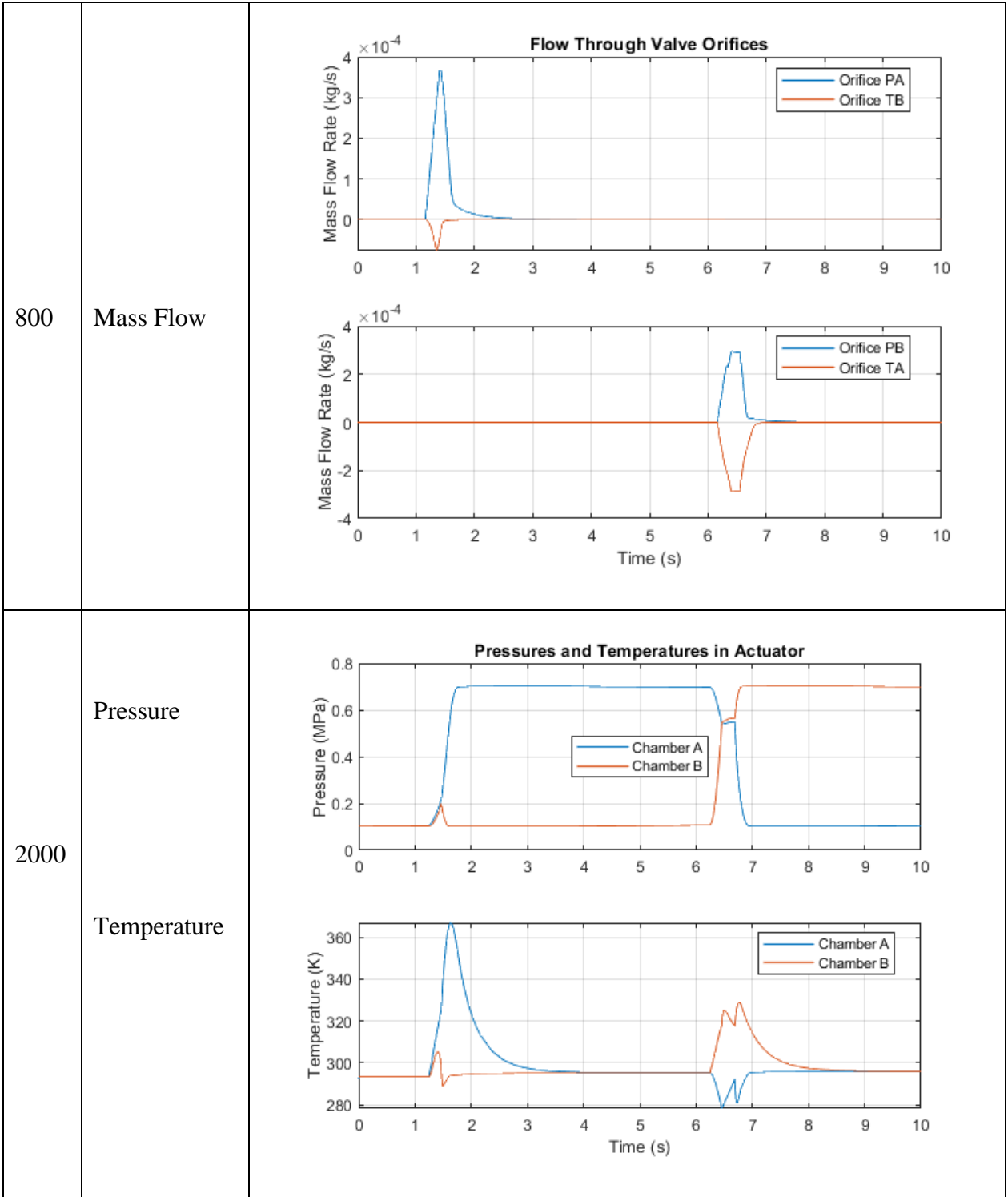
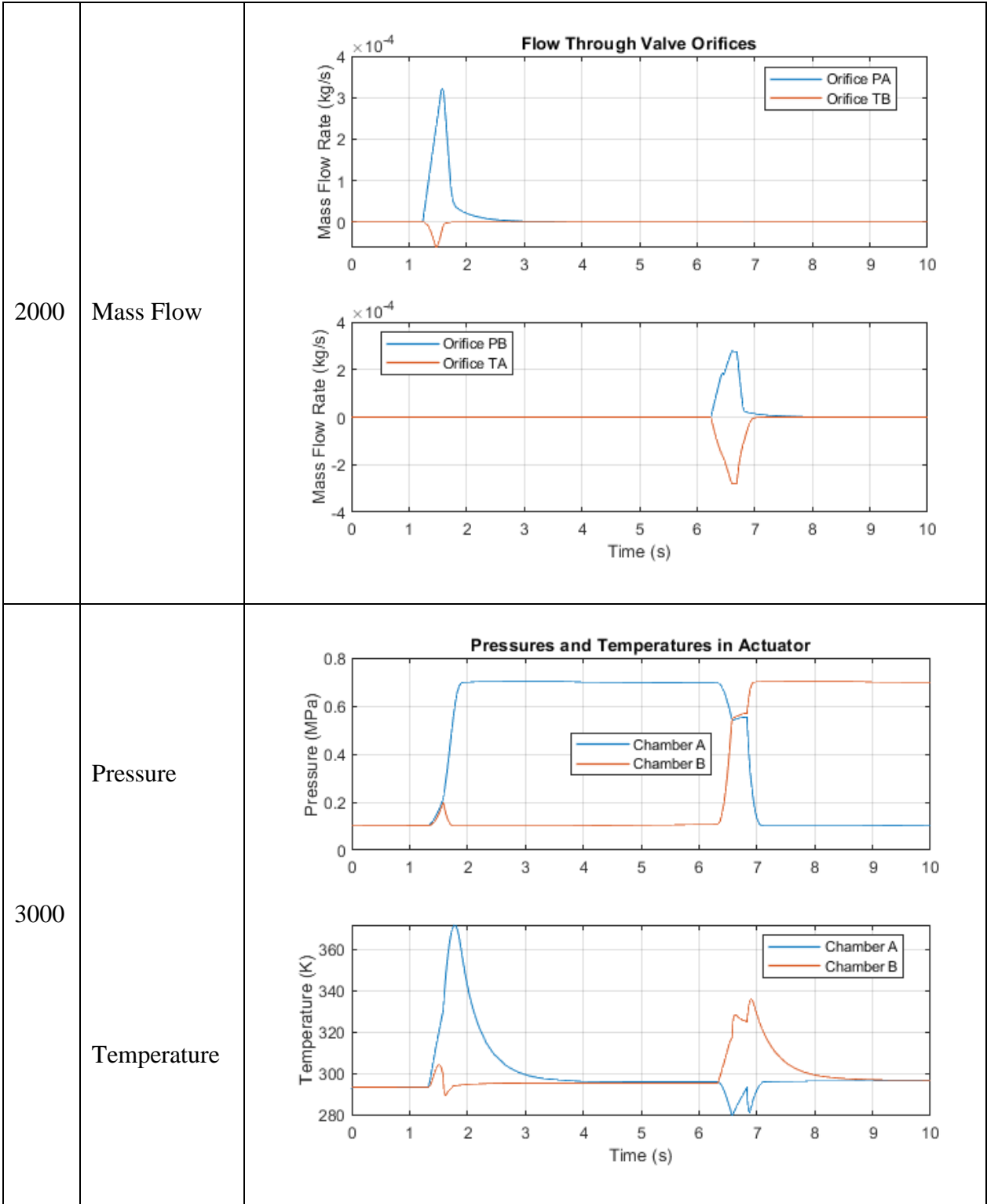
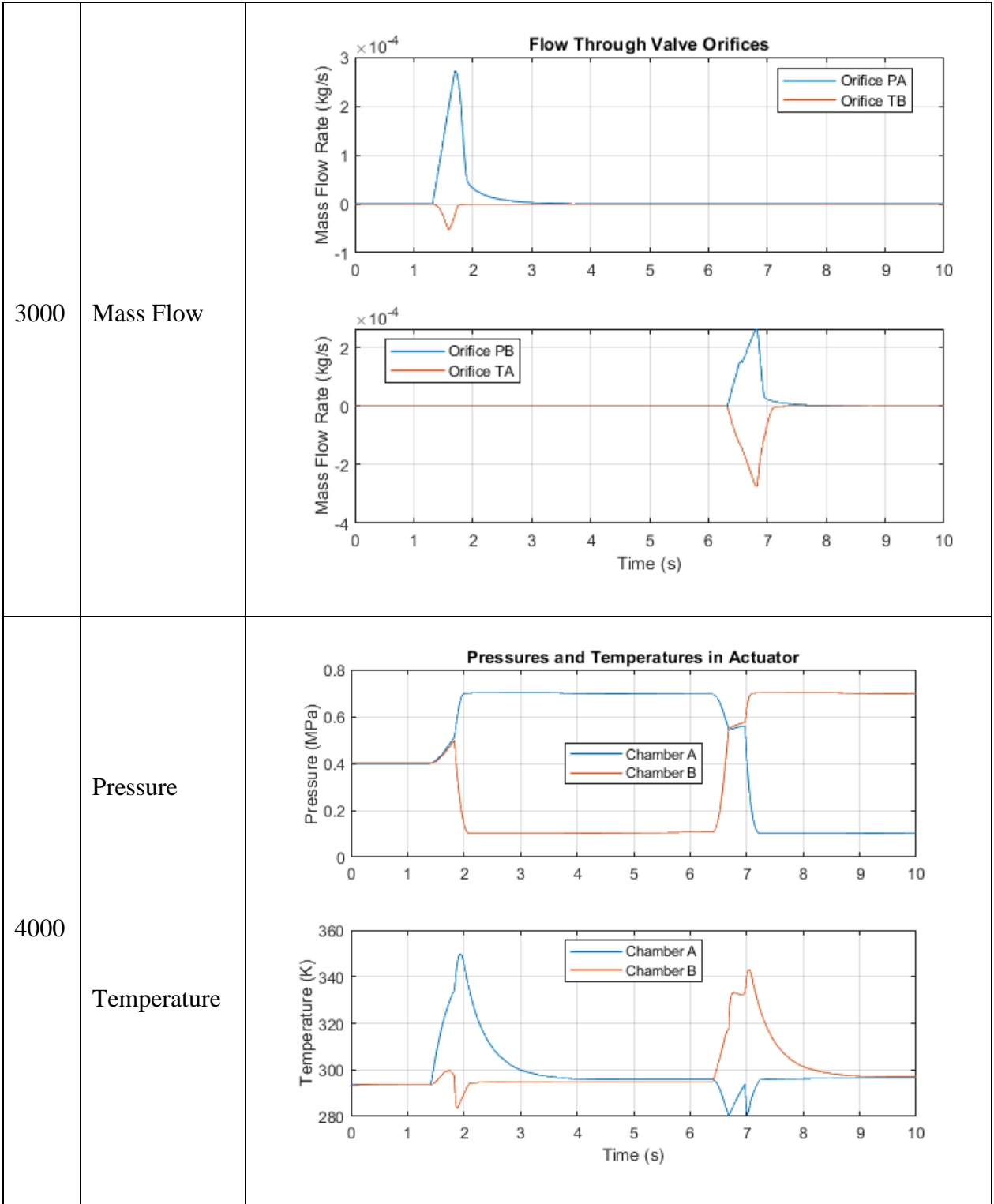


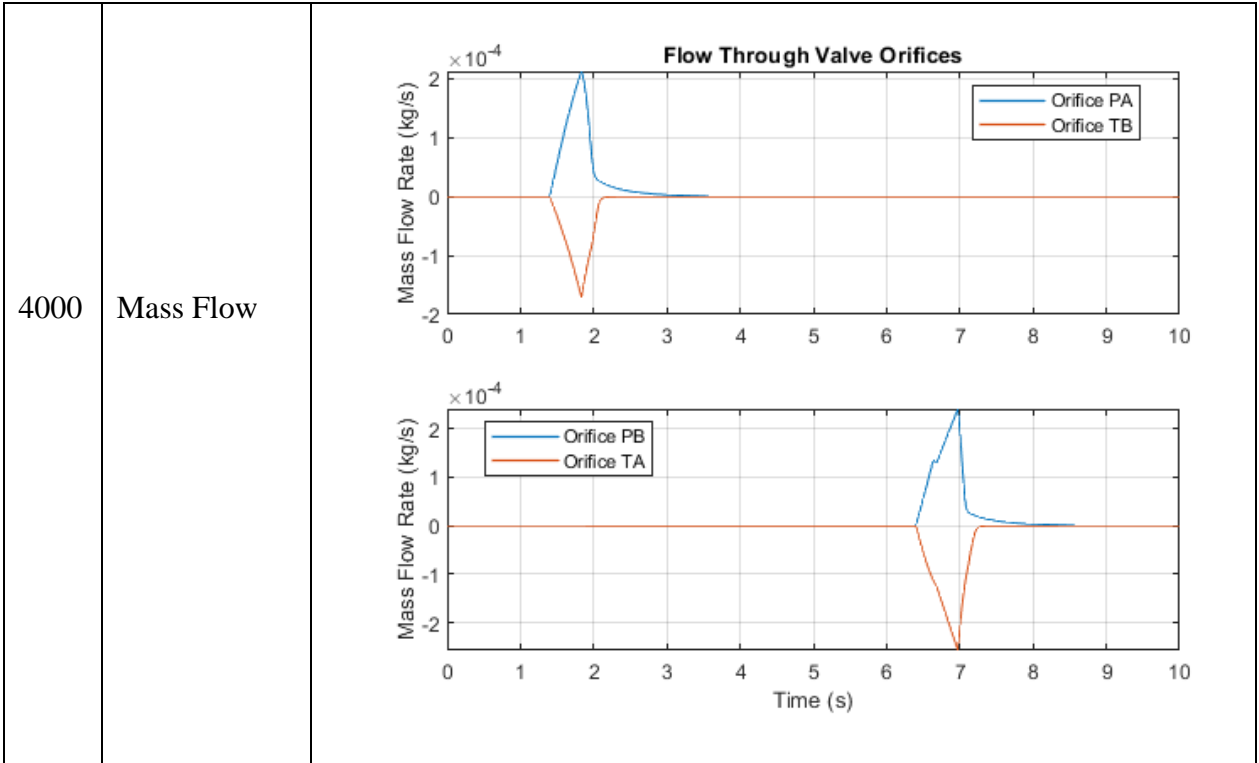
Table 11: Parametric Results 1



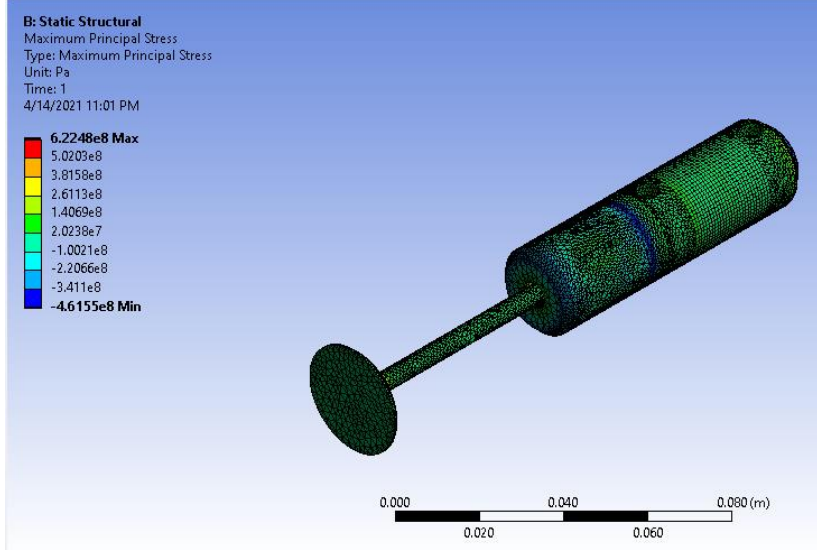


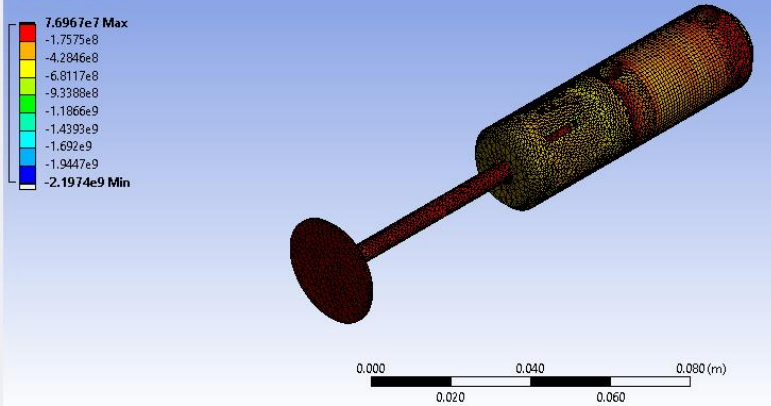
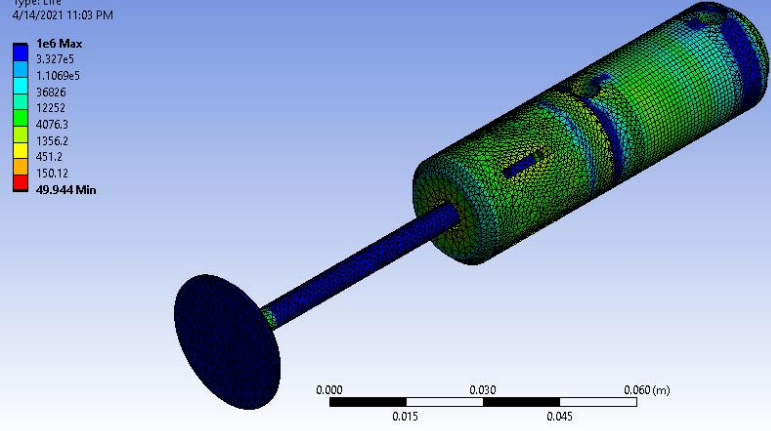
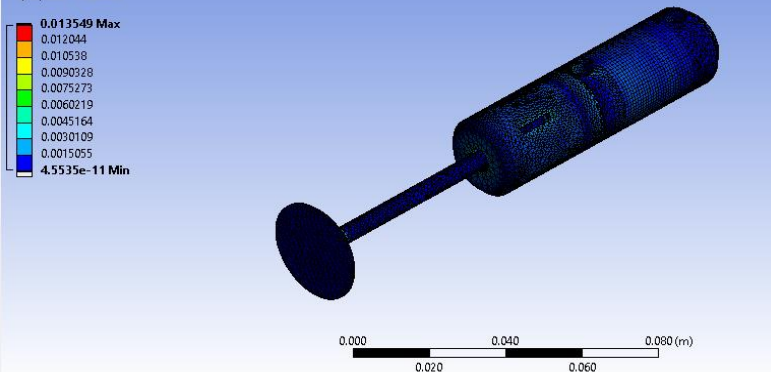






Structural Analysis

Component	Analysis Parameter	Results
	Maximum Principal Stress	<p>B: Static Structural Maximum Principal Stress Type: Maximum Principal Stress Unit: Pa Time: 1 4/14/2021 11:01 PM</p>  <p>6.2248e8 Max 5.0203e8 3.8150e8 2.6113e8 1.4069e8 2.0230e7 -1.0021e8 -2.2066e8 -3.411e8 -4.6155e8 Min</p> <p>0.000 0.020 0.040 0.060 0.080 (m)</p>

	<p>Minimum Principal Stress</p>	<p>B: Static Structural Minimum Principal Stress Type: Minimum Principal Stress Unit: Pa Time: 1 4/14/2021 11:01 PM</p> 
<p>Actuator</p>	<p>Fatigue Life</p>	<p>B: Static Structural Life Type: Life 4/14/2021 11:03 PM</p> 
	<p>Equivalent Total Strain</p>	<p>B: Static Structural Equivalent Total Strain Type: Equivalent Total Strain Unit: m/m Times: 1 4/14/2021 11:02 PM</p> 

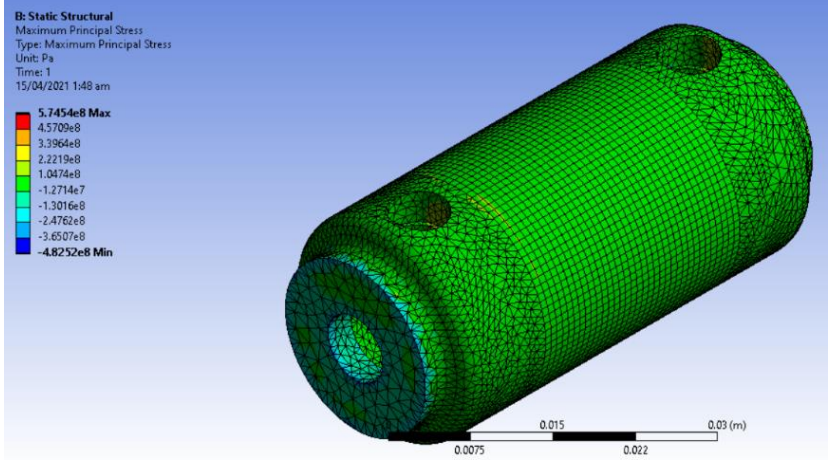
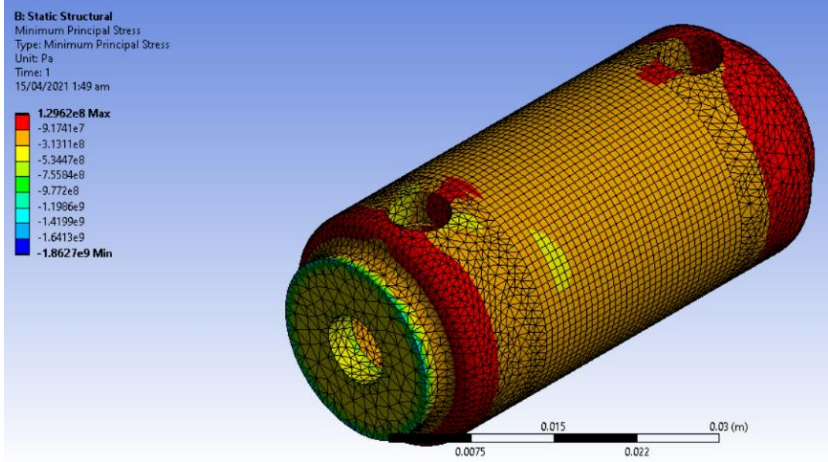
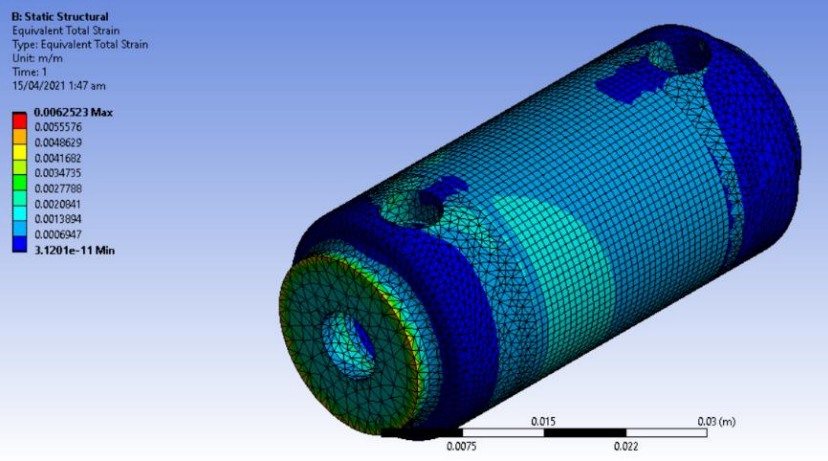
	<p>Maximum Principal Stress</p>	 <p>B: Static Structural Maximum Principal Stress Type: Maximum Principal Stress Unit: Pa Time: 1 15/04/2021 1:48 am</p> <p>5.745e8 Max 4.5709e8 3.3964e8 2.2219e8 1.0474e8 -1.2714e7 -1.3016e8 -2.4762e8 -3.4507e8 -4.8252e8 Min</p>
<p>Pressure Chamber</p>	<p>Minimum Principal Stress</p>	 <p>B: Static Structural Minimum Principal Stress Type: Minimum Principal Stress Unit: Pa Time: 1 15/04/2021 1:49 am</p> <p>1.2962e8 Max -9.1741e7 -3.1311e8 -5.3447e8 -7.5594e8 -9.772e8 -1.1986e9 -1.4199e9 -1.6413e9 -1.8627e9 Min</p>
	<p>Equivalent Total Strain</p>	 <p>B: Static Structural Equivalent Total Strain Type: Equivalent Total Strain Unit: m/m Time: 1 15/04/2021 1:47 am</p> <p>0.0062523 Max 0.0055576 0.0048629 0.0041682 0.0034735 0.0027788 0.0020841 0.0013894 0.0006947 3.1201e-11 Min</p>

Table 12: Parametric Results 2

CFD ANALYSIS

Component	Analysis Parameter	Results
Double Acting Actuator	Velocity	<p>Velocity Contour 2 2.645e+02 2.442e+02 2.238e+02 2.035e+02 1.831e+02 1.628e+02 1.424e+02 1.221e+02 1.017e+02 8.139e+01 6.105e+01 4.070e+01 2.035e+01 0.000e+00 [m s⁻¹]</p>
	Pressure	<p>Pressure Contour 1 3.675e+04 3.266e+04 2.856e+04 2.446e+04 2.036e+04 1.626e+04 1.217e+04 8.067e+03 3.968e+03 -1.295e+02 -4.228e+03 -8.326e+03 -1.242e+04 -1.652e+04 -2.062e+04 -2.472e+04 -2.882e+04 [Pa]</p>
	Velocity	<p>Velocity Volume Rendering 1 2.645e+02 1.984e+02 1.323e+02 6.613e+01 0.000e+00 [m s⁻¹]</p>

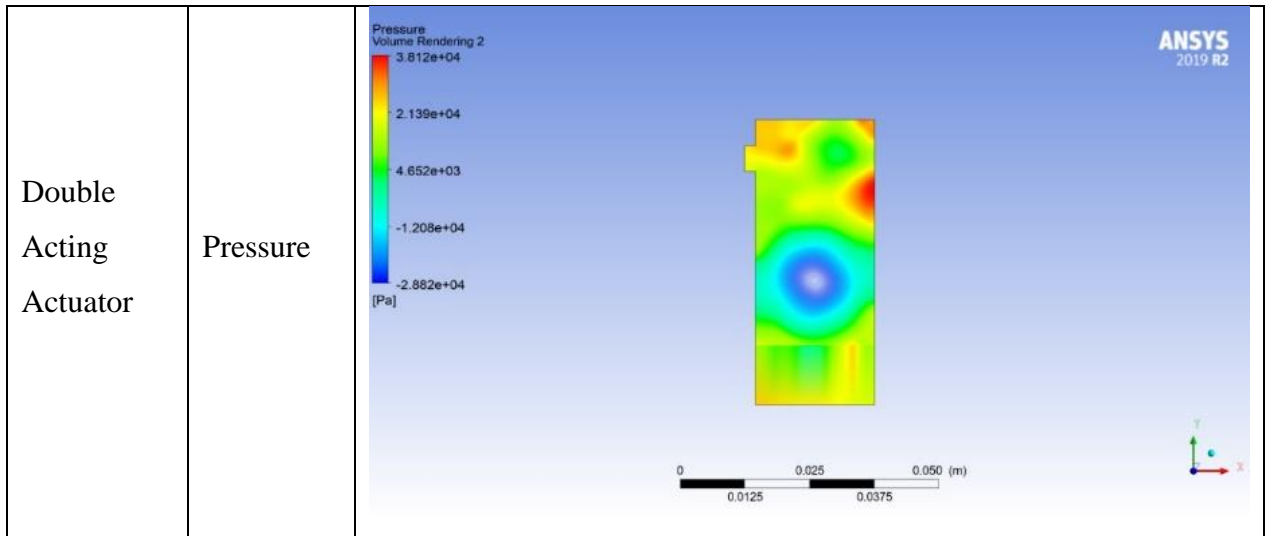


Table 13: Parametric Results 3

4.2 SIMULINK DISCUSSION

The close analysis of the results obtained from Simscape helps us understand the velocity profile in the orifices. This also presents us the pressure and temperature variation in the orifices. The working pressure for the double acting actuator is 8 bar and the maximum temperature is around 370 K. We need to make sure in our manufacturing plan that the design accommodates these working conditions. The mass flow rate variation will be required for analysis in CFD and makes sure that we know the optimal value of mass flow rate and pressure for our reservoir. If the actuator falls short of the pressure and required mass flow rate, the actuator will not work

4.3 CFD Discussion

The dynamic mesh was implemented in the CFD Analysis. The analysis is displayed in terms of the pressure and velocity contours. The velocity profile suggests that air flows into the chamber and pushes the piston forwards. The velocity data helps us in broader understanding of the flow characteristics and design improvement.

While SIMULINK data helps us understand the flow characteristics in the pipe network, CFD analysis presents us the velocity profiles inside the flow chamber. The air having a specific mass flow rate moves from an orifice into the chamber and manifests a profile.

The analysis was done for the forward stroke only. It is recommended through observations that geometry used for the actuator should have round off edges and dead space must be negligible. This will have improvement in amount of fluid flow rate passing through the actuator. We can use CFD in optimized model of the actuator. It is also proposed to model the analysis using correct turbulence model which fits the right solution.

4.4 FEM Discussion

Under the optimal boundary conditions and a fine operational mesh, we have the desired values for stresses and strains in the double acting actuator. The analysis was done in order to validate the design specifications. The maximum stress of 135 MPa lies within the elastic limit. Our data shows that there is no failure or fracture in any component of the actuator. Instead, the stresses and strains are in an appreciable range which accounts to proper design of the product. The product has to endure a lot of cyclic loading and our fatigue analysis suggests that this product is perfectly designed for this purpose. There is very less significant deformation in the components which suggests that product can work under the provided operating conditions.

Component	Material	Tensile strength (MPa)	Yield strength (MPa)	Max stress of FEM analysis (MPa)
Pressure chamber	Stainless Steel Grade 304	505	215	129.6
Plunger	Stainless Steel Grade 304	505	215	88.59
Spring housing	Stainless Steel Grade 304	505	215	66.82

Table 14: Quantitative FEM Results

Component	Maximum Stress	Maximum Deformation
Actuator	105.39 MPa	0.00011055 m
Plunger	62.12 MPa	2.0137 e -4 m
Valve	66.37 MPa	1.058 e-4 m
Main Housing	55.57 MPa	0.00022778

Table 15: Maximum Stresses and Deformation

CHAPTER 5 : MANUFACTURING PLAN

5.1 Manufacturing Processes

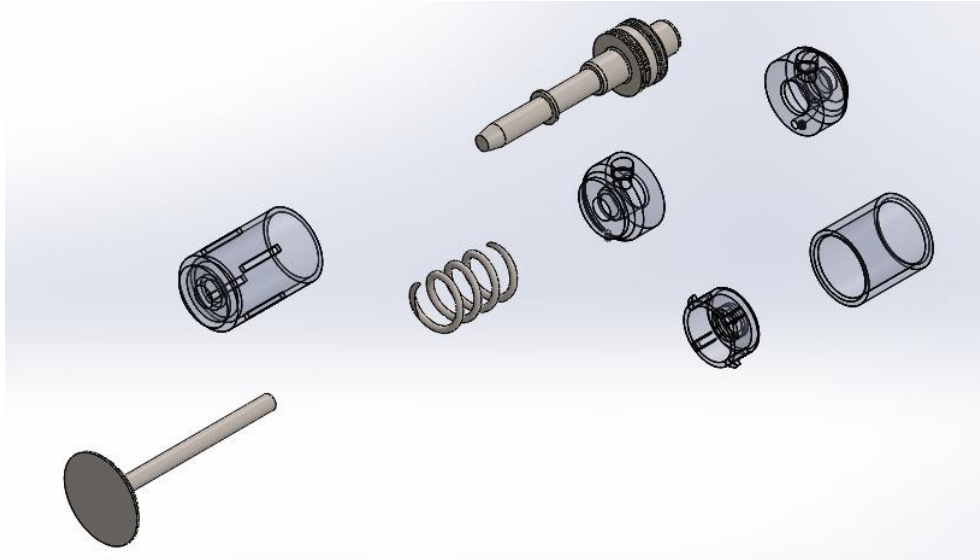


Figure 41: Exploded View of Actuator

The different parts shown in figure 41 are manufactured according to the dimensions and peak working conditions mentioned in the methodology section.

The manufacturing processes include:

- **Upsetting process** for engine valve

Raw materials are received in the form of long cylindrical bars which are cut to required sizes. The parts are then forged by a hydraulic press to give them the valve head shape. The forged head and stem are joined by TIG welding process, after which the valve is machined for a better finish and heat treated to improve physical properties. Surface treatments are also done including an alkaline bath.

- **Machining process** for actuator piston

The actuator piston is manufactured using a lathe machine. The piston starts out as a metal rod of a specific diameter and length, outer step turning is done to achieve required diameters along the length of the rod. The ends are squared and

chamfering done where necessary. Grooving is done into the diaphragm of the piston to incorporate pneumatic seals and lubrication.

The valve and piston are fastened together using threads, to aid in disassembling the actuator from the valve for maintenance.

- **Machining** for Pressure chamber

The pressure chamber is divided into three sections, one center cylindrical body and two end bodies.

The main cylindrical body is manufactured on the lathe machine, by facing a cylindrical bar to the given length and boring done to remove material from the inside. Boring done to the point where thickness of the cylinder reaches required value.

Same is done for the chamber's ends. Holes are drilled into them on a milling machine which act as inlet ports for compressed air and a passage through which the piston moves. Threading is done to couple these parts together in a non-permanent fashion for future maintenance.

- **Machining** for spring housing

The spring housing consists of an internal and external holder to guide motion of spring and prevent buckling. They are manufactured using the same principle as the pressure chamber, intermeshing grooves are incorporated to guide the motion.

5.2 Pneumatic Components

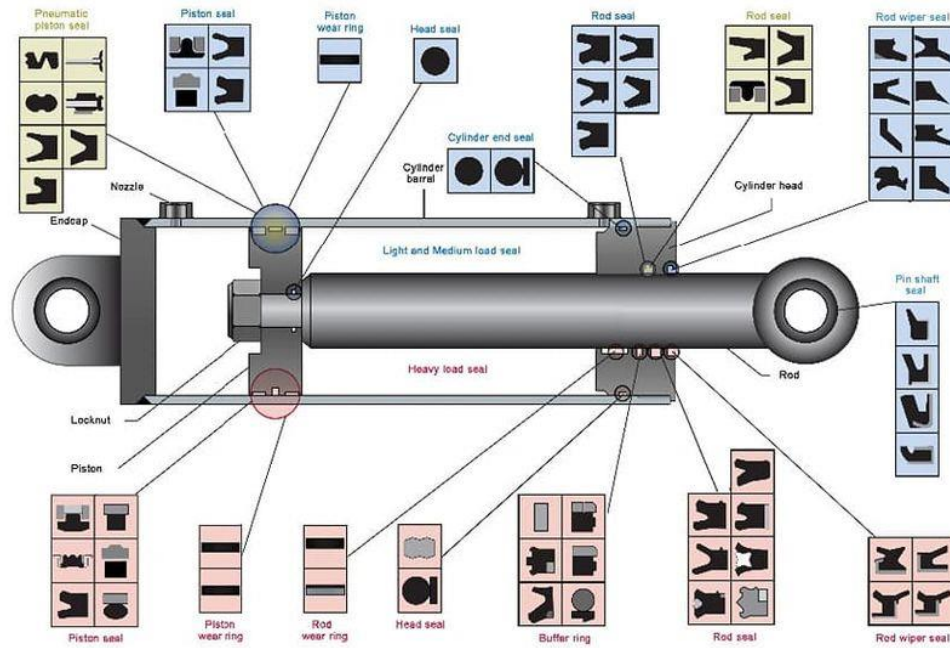


Figure 42: Pneumatic Seals

Type of Seal	Description	Sample Seal Material	Working Pressure /MPa	Working Temperature /C
Pipe Fittings	Connect different pneumatic components	PTFE	5	-30 - 200
Piston Seal	Maintain lubricating film and minimize friction	PTFE	5	-30 - 200
Rod Seal	Maintain lubricating film and minimize friction	Polyurethane	1.6	-30 - 100
Cushioning	Designed for pneumatic cushioning where high pressure peaks occur	Polyurethane	1.6	-35 - 110
Wear Rings	Guiding the piston in a cylinder and of absorbing transversal forces in it	Polyurethane	-	-40 - 110
Static	For pipe fittings and stationary fittings	TPU	1.0	-10 - 60
Wiper Seals	Prevent ingress of contaminated particles into dynamic rod guides	TPU	-	-35 - 90

Table 16: Pneumatic Seal Selection

5.3 Sensors

5.3.1 Position Sensors

Pneumatic cylinders require linear position sensors where a position feedback is crucial. All available sensors include use of a magnetic field to provide position feedback. A magnet is internally incorporated into the pneumatic cylinder and a sensor mounted on the body. There are a lot of criteria to choose a sensor best suited for the give working conditions which include working environment, signal switching speed, mounting, robustness etc.

Considering all judging criteria as shown in Table, a GMR type position sensor was chosen as it provides better

Robustness, high switching speeds, low power consumption and high temperature stability. All of which are suited for the sensor to be applied in the harsh working environment surrounding an engine.

	Reed Switch	Hall Effect	AMR	GMR
Size	Large	Small	Medium	Small
Cost				
Magnetic Strength	Medium	High	Low	Low
Sensitivity	Medium	Low	High	High
Temperature Stability	Medium	Low	Medium	High
Power Consumption	Zero	Low	High	Low
Noise Immunity	High	Low	High	High
Mechanical Robustness	Low	Medium	High	High
Electrical Robustness	Low	Low	High	High
Switching Speed	Low	High	High	High

Table 17: Position Sensor types

5.3.2 Optical Encoder

The main input of the proposed system is crank angle degree (CAD). This sensor input provides system with a value showcasing angular position of the crank shaft, then outputs the corresponding programmed linear displacement of the pneumatic actuator at the point in time.



Figure 43: Optical Encoder

The shaft is directly connected to the crank shaft in the axial direction. An absolute type encoder is being used that provides true position of the crank instead of a relative type.

Working parameters of the encoder are given in table ____.

Type	Parameter	Range
Environmental	Temperature	-25 - 85 Celsius
Mechanical	Max shaft speed	7000 RPM
Mechanical	Acceleration	100000 rad/sec
Electrical	Voltage	12V
Electrical	Absolute Accuracy	0.18 Degree
Electrical	Position Update	7ms
Electrical	Power Drain	18.5 mA

Table 18: Optical Encoder Working Conditions

5.3.3 Pressure Sensor

As the whole pneumatic system works on the basis of compressed air and pressures at different points along the circuit, it is important to incorporate pressure sensors. These pressure sensors will provide information to the control unit whether the system is working under optimal pressures. Ceramic (piezo-electro) sensing elements provide high burst/overpressure protection, while stainless steel welded thin-film sensing elements provides very fast response time.

Housing Material	Stainless Steel
Operating Temperature	-40 - 90 Celsius
Protection	IP69K
Accuracy	0.5%
Operating Voltage	8.5 – 36V
Step Response Time	1ms
Maximum Sensing Pressure	12 bar

Table 19: Pressure Sensor Working Conditions



Part No. SPTD25-20-0100H

Figure 44: Pressure Sensor

5.4 Cost Analysis

Sr. No	Name of the Hardware	Quantity	Specifications	Role in the Project	Price (PKR)
1	Arduino Controller	1	14 Digital I/O 6 Analog I/O 32 Kb Flash Memory and a serial port	Works as a controller in the system which accepts signal from MATLAB	550
2	Relay Unit (4 channel)	1	+12 Volts , 10 Amp current capacity , 1 NO and NC contact	Accepts signals from Arduino and passes to solenoid valve	570
3	Pneumatic Actuator	4	Double Acting Actuators , 11.63 mm stroke and 1" bore	Actuators according to the air flow provided by the valves	12000
4	Solenoid Valve	4	4/3 DCV , single side solenoid and Spring return (+12 volts and 150 mA)	Passes compressed air towards the Actuators	18000
5	Compressor	1	8 bar working pressure , 1 phase 220 volts 10 Amp	Compresses air for the pneumatic system	20000
6	Encoder	1	Type 2614D21	Finds crank angle	1500
7	Transistor	1	TIP122 Darlington's Transistor	Operates the solenoid of DCV	
8	Optocoupler	1	TLP250	Light dependent electricity transfer	120
9	Voltage regulators	2	LM 7824 and LM 7805	Maintain a constant voltage	3000
10	FRL unit	1	Type OU-MINI-3/8	Ensure clean air in a pneumatic system	9500
11	Pressure Gauge	1	Type T5500	Analysis of an applied force by a fluid on a surface	7200
12	Circuit board components		LEDs, Power MOSFETS, Resistors, Diodes, wires	Used for electronic circuit	200
13	Arduino Uno Shield	1	SKU AR496OT1IEMJQNAFAMZ-3269514	used for mounting/soldering all circuit components	300
14	Soldering iron and solder	1	SKU 167116596_PK-1335408572	Used for electrical connections	2500
15	Motor controller with dial/knob	1	digital potentiometer with switch 5Pin 3Pin	essentially a voltage divider used for measuring electric potential (voltage)	20
16	Flywheel diode	1	1N4001	prevent back emf which can damage the controller setup	20

CHAPTER 6 : CONCLUSIONS AND RECOMMENDATIONS

An electro pneumatic variable valve actuation system was developed for a camless engine. Initial development and calculations confirmed its functional ability to control the valve timing, lift, velocity, and event duration on different set of rpms. The electro pneumatic valve train is integral with the cylinder head, which lowers the head height and improves the engine packaging. The modified engine is light weight and smaller in size, making this product a very fine addition to engineering world.

The design and calculations complement the CFD analysis and FEM analysis. The calculations were done using the real-life data and implemented into SIMULINK analysis. Our design is robust, and the calculations show that the design works well at high rpms like 4000 without failure in components. The design is entirely simple and works well with the control system. Pneumatic system can easily be controller using MATLAB Simulink and Arduino controller

The design of actuators and actuating system is entirely theoretical, so we can't predict the exact working of the model in real life, but it does lay foundation to manufacturing of VVT system

Here are the some of the recommendations we are proposing based upon the findings and calculations.

- Design can be used to make high pneumatic force controller to manage the pneumatic system.
- In order to improve the working performance of the system, PID controller can be used.
- Online monitoring system can be used using Internet of things to monitor the system remotely.

- As for further research, there is gap for electric components, electric circuits, design and development of solenoids, control valves and selection of appropriate pressure source.
- The analysis for better estimates can be done in future in 3D working environment with more understanding of meshes and boundary conditions. This will lead to better results.

Presently many automobile makers like Fiat, BMW and TATA motors are doing research to develop this technology. Further research and development are needed in this domain to take full advantage of this system's exceptional flexibility. The system looks revolutionary in diesel and petrol engines

Automobiles but however exemplary this system looks, implementation of the project into a real life working model is a big challenge for the automobile industry.

Camless engine also has scope in stationary engines because of less vibrations. As the camless engine removes all the disadvantages of cam engine it also developed for application in aerospace

Some of the benefits in a camless engine are substantial improvements in performance, fuel economy, and emissions. The development of a camless engine with an electro pneumatic valve train described in this report is only a first step towards a complete engine optimization. Further research and testing of the model is necessary to make a real life and working prototype, ready to perform in automobiles. The project has never ending research needed to get a highly functional system and works closely to the theoretical values.

REFERENCES

- [1] MAN B&W Diesel Engines. (2003). Camless two stroke main propulsion engine. Camless two stroke main propulsion engine.
- [2] Hong, H. (2004). Review and analysis of variable valve timing strategies - eight ways to approach. Proceedings of the Institution of Mechanical Engineers, Part D: Journal of Automobile Engineering, 218(10), 1179–1200.
- [3] Wu, B. (2007). A simulation-based approach for developing optimal calibrations for engines with variable valve actuation. Oil and Gas Science and Technology.
- [4] Jia Ma, Guoming Zhu (2008) ELECTRO-PNEUMATIC EXHAUST VALVE MODELING AND CONTROL FOR AN INTERNAL COMBUSTION ENGINE.
- [5] "Valeo tests camless system for gas engines; supplier hopes to produce fuel-saving technology by '08: AutoWeek Magazine". Autoweek.com. 2009-02-06. Archived from the original on 2011-05-22. Retrieved 2009-10-02.
- [6] Lou, Zheng David; Deng, Qiangquan; Wen, Shao; Zhang, Yunhai; Yu, Mengjin; Sun, Ming; Zhu, Guoming (2013). "Progress in Camless Variable Valve Actuation with Two-Spring Pendulum and Electrohydraulic Latching". SAE International Journal of Engines.
- [7] Modeling and Verification of Valve Train Dynamics in Engines by M Husselman (2015)
- [8] Travis Okulski (26 February 2014). "What It's Like To Ride In A Car With The Camless Engine Of The Future". Jalopnik. Retrieved 5 June 2016.
- [9] Aliyu Bhar Kisabo (2017) Comparative Analysis Between Cam and Cam-less Valve Actuating for Automotive System
- [10] M.Jimenez, E. Kurmyshev (2020) Experimental Study of Double-Acting Pneumatic Cylinder

[11] Modeling and Dynamic Analysis on the Direct Operating Solenoid Valve for Improving the Performance of the Shifting Control System Xiangyang Xu^{1,2}, Xiao Han^{1,2}, Yanfang Liu^{1,2,*}, Yanjing Liu^{1,2} and Yang Liu³ (2017)

[12] Design and Performance Evaluation of an Electro-Hydraulic Camless Engine Valve Actuator for Future Vehicle Applications Kanghyun Nam^{1, †}, Kwanghyun Cho^{2, †}, Sang-Shin Park¹ and Seibum B. Choi³

APPENDIX I: SENSOR TECHNOLOGY



AAH Sensors

AAH Sensors

Features:

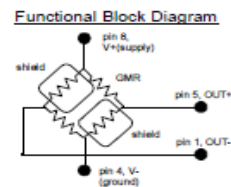
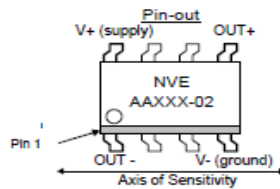
- Extremely High Sensitivity to Applied Magnetic Fields
- Wheatstone Bridge Analog Output
- Temperature Tolerance to 150°C Continuous
- Near-Zero Voltage Operation
- DC to >1MHz Frequency Response
- Small, Low-Profile Surface Mount Packages

Applications:

- Low Voltage, High Temperature Applications
- Low Field Sensing for Magnetic Media Detection
- Earth's Magnetic Field Detection
- Current Sensing

Description:

The AAH-Series GMR sensors are manufactured with a high sensitivity GMR material, making them ideally suited for any low magnetic field application. They are also extremely temperature tolerant, to +150°C operating temperatures.



Magnetic Characteristics:

Part Number	Saturation Field (Oe ¹)	Linear Range (Oe ¹)		Sensitivity (mV/V-Oe ¹)		Resistance (Ohms)	Package ²	Die Size ³ (μm)
		Min	Max	Min	Max			
AAH002-02	6	0.6	3.0	11.0	18.0	2K ±20%	SOIC8	436x3370
AAH004-00	15	1.5	7.5	3.2	4.8	2K ±20%	MSOP	411x1458

NITRA CPS9D Series Cylinder Switch Specifications	
Operating Voltage	5-28 VDC
Voltage Drop	1.0 V
Current Rating	0.2 Amps Max.
Wire Size	26AWG (0.13mm ²)
Switching Power	4.8 watts Max.
Switching Speed	4μs operate / 4μs release
Short Circuit Protection	No
Reverse Polarity Protection	Yes
Overload Protection	No
Leakage Current	< 0.01 mA
Sensing Technology	GMR
Off Delay Time	150-200 ms
Function Display	PNP switching status yellow / NPN switching status red
Switching Frequency	< 1000 Hz
Magnetic Sensitivity	2.5 millitesla (25 gauss)
Housing Materials	Zytel
Operating Temperature	-4°F to 176°F (-20°C to 80°C)
Protection Rating	NEMA 6 / IP 67
Agency Approvals	CE, RoHS, REACH

APPENDIX II: Compression Spring Specifications

Compression Spring



sales@accessspring.com
Ph 951 276 2777

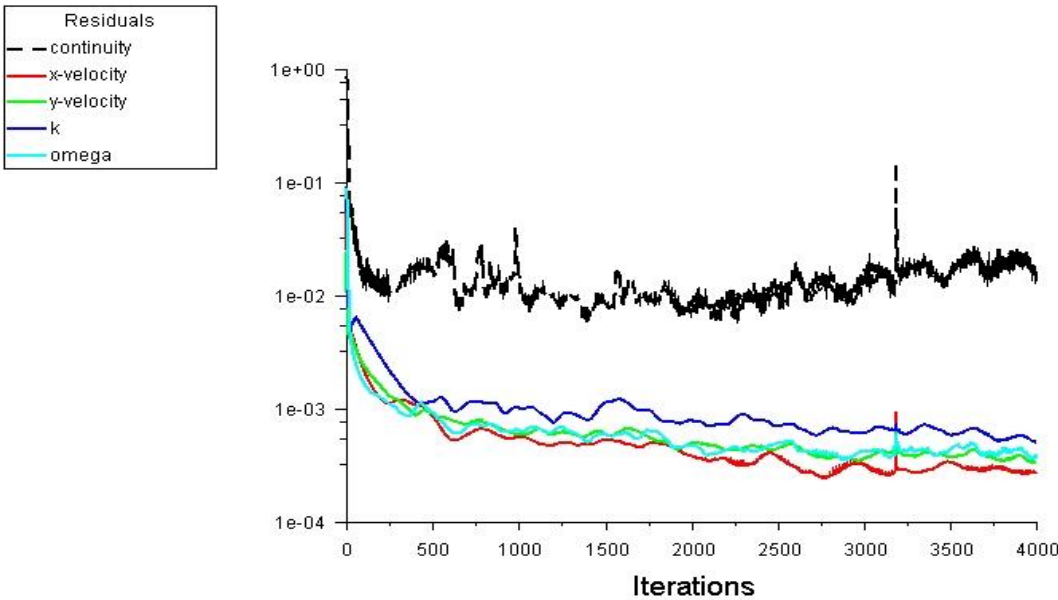
Part #: AC4900-38000-5.000-HD-40.400-CG-N-MM

Physical Dimensions:	Tolerances:
Wire Diameter:	4.900 mm +/- 0.0254
Outer Diameter:	38.000 mm +/- 1.016
Inner Diameter:	28.200 mm +/- 1.016
Free Length:	40.400 mm +/- 1.27
Active Coils:	3.000 +/- 1/4 coil
Total Coils:	5.000 +/- 1/4 coil
Solid Height:	24.5 mm +/- 1.715
End Type:	Closed & Ground
Spring Index:	6.755
Spring Rate:	52.482 N/mm +/- 5.248
Maximum Load:	711.040 N +/- 71.104
Maximum Travel:	135.48 mm
Load 1:	200.000 N @ 36.589 loaded height



Part Name:	Revision #:	Approved by:
Material: Hard Drawn MB ASTM A227	Scale: 1.27	Drawn by:
Finish:		Date Drawn: 04 / 13 / 2021
Tolerances:		*Ref. to meet Rate or Loads

APPENDIX III: CFD Convergence Results



APPENDIX IV: GOODMAN FAILURE DIGRAM

